Supplement of Atmos. Chem. Phys., 17, 5583–5599, 2017
http://www.atmos-chem-phys.net/17/5583/2017/
doi:10.5194/acp-17-5583-2017-supplement

Atmospheric Chemistry and Physics Open Access EGU

Supplement of

Influence of organic compound functionality on aerosol hygroscopicity: dicarboxylic acids, alkyl-substituents, sugars and amino acids

Aleksandra Marsh et al.

Correspondence to: Jonathan P. Reid (j.p.reid@bristol.ac.uk)

Table S0 Parameters required for thermodynamic model predictions (* available from a predefined list). And contents of supplement by page and S number.

Compound	Molar Mass / g.mol $^{-1}$	UNIFAC Structure	Page and S No
DL- Alanine	89.09	CH_3 COOH $CHNH_2$	P3 S1
L-Asparagine	132.12	COOH CH_2 $CONH_2$	P38 S36
L-Aspartic Acid	133.10	CH_2 $(COOH)_2$ $CHNH_2$	P37 S35
L-Arginine	174.2	-	P4 S2
Glycine	75.06	COOH CHNH2	P5 S3
L-Histidine	155.15	-	P6 S4
L-Lysine	146.19	COOH $CHNH_2$ $(CH_2)_3$ CH_2NH_2	P7 S5
L-Proline	115.13	-	P8 S6
L-Threonine	119.12	OH CH_3 CH COOH $CHNH_2$	P9 S7
L-Valine	117.15	$(CH_3)_2$ CH COOH $CHNH_2$	P10 S8
Oxalic Acid*	90.03	$(COOH)_2$	P13 S11
Malonic Acid*	104.062	$(COOH)_2CH_2$	P14 S12
Succinic Acid*	118.09	$(COOH)_2$ $(CH_2)_2$	P15 S13
Methyl Malonic acid		$(CH_3)(CH)(COOH)_2$	P19 S17
Glutaric Acid*	132.116	$(COOH)_2$ $(CH_2)_3$	P16 S14
Methyl Succinic Acid*		$(CH_3)(CH_2)(CH)(COOH)_2$	P20 S18
Dimethyl Malonic Acid		$(CH_3)_2(C)(COOH)_2$	P36 S34
Adipic Acid*	146.14	$(COOH)_2$ $(CH_2)_4$	P17 S15
2-Methyl Glutaric Acid*		$(CH_3)(CH_2)_2(CH)(COOH)_2$	P24 S22
3-Methyl Glutaric Acid*		$(CH_3)(CH_2)_2(CH)(COOH)_2$	P26 S24
2,2-Dimethyl Succinic Acid*		$(CH_3)_2(CH_2)(C)(COOH)_2$	P23 S21
2,3-Dimethyl Succinic acid		$(CH_3)_2(CH)_2(COOH)_2$	P35 S33
Pimelic Acid	160.17	$(COOH)_2$ $(CH_2)_5$	P18 S16
2,2-Dimethyl Glutaric Acid		$(CH_3)_2(CH_2)_2(C)(COOH)_2$	P22 S20
3-Methyl Adipic Acid		$(CH3)_1(CH2)_3(CH)(COOH)_2$	P25 S23
3,3-Dimethyl Glutaric Acid		$(CH_3)_2(CH_2)_2(C)(COOH)_2$	P27 S25
Diethyl Malonic Acid		$(CH3)_2(CH2)_2(C)(COOH)_2$	P21 S19
Citric Acid*	192.12	$(COOH)_3$ $(CH_2)_2$ $C^{(OH)}$	P11 S9
Tartaric Acid	150.09	$(COOH)_2$ $(OH)_2$ $(CH)_2$ $^{(OH)}$	P12 S10
Sorbitol	182.17	$(CH_2^{[alc]})_2$-$(CH_1^{(OH)})_4$ $(OH)_6$	P31 S29
D-(+)-Trehalose Dihydrate	378.33	(CH) $(CH_2^{[OH]})_8(CHO^{[ether]})_3$ $(OH)_8$	P32 S30
Galactose	180.16	CHO $(CH_1^{(OH)})_4$ $CH_2^{(alc)}$ $(OH)_5$	P33 S31
Xylose	150.13	$(CH_2(OH))_3$ $CH_2^{(alc)}$ CHO $(OH)_4$	P34 S32
PEG4	194.23	$(OH)_2$ $(CH_2O)_3$ $(CH_2)_3$ $(CH_2^{(OH)})_2$	P29 S27
PEG3	150.17	$(OH)_2$ $(CH_2)_2$ $(CH_2O)_2(CH_2^{(OH)})_2$	P28 S26
Erythritol	122.12	$(CH^{(OH)})_2$ $(CH_2^{(OH)})_2$ $(OH)_4$	P30 S28

Table S0.1 Fitted parameters for upper and lower MFS vs water activity of compounds in each class, amino and organic acids, sugars and alcohols, as shown in Figure 11b) in the manuscript. The power law coefficient P is used to calculate energy parameter C for the first to $(n-1)$th layers, hence $C_i = (i/n)^P$, where i is the layer number and n is the total number of hydration layers, here $n = 8$ for all compounds except glycine ($n = 3$) and 2,2-dimethyl glutaric acid ($n =$

16). MSE is a normalized mean-square error, equal to $\left(\frac{1}{n_p}\right)\sum_{i=1}^{n_p}((m_{model,i}-m_{data,i})/(m_{model,i}))^2$, where n_p is the number of data points.

Solute	*P*	MSE
Amino acid Upper (Glycine)	-1.934	0.00321
Amino acid Lower (Asparagine)	-0.171	0.04151
Organic acid Upper (Malonic acid)	-0.212	0.00819
Organic acid Lower (2,2 dimethyl glutaric acid)	0.206	0.08315
Sugar Upper (Sorbitol)	-0.522	0.01025
Sugar Lower (Trehalose)	-0.870	0.01687
Alcohol Upper (Erythritol)	-0.238	0.01311
Alcohol Lower (PEG4)	-1.180	0.16205

Table S0.2 Fitted parameters for nine amino acids. The power law coefficient *P* is used to calculate energy parameter *C* for the first to $(n-1)$th layers, hence $C_i=(i/n)^P$, where *i* is the layer number and *n* is the total number of hydration layers, here $n = 8$ for all compounds except glycine ($n = 3$) and threonine ($n = 5$). MSE is a normalized mean-square error, equal to $\left(\frac{1}{n_p}\right)\sum_{i=1}^{n_p}((m_{model,i}-m_{data,i})/(m_{model,i}))^2$, where n_p is the number of data points. (Parameter for L-aspartic acid could not be determined due to data range available.)

Solute	*P*	MSE
Alanine	-0.356	0.00051
Asparagine	-0.171	0.04151
Arginine	-0.993	0.04039
Glycine	-1.934	0.00321
Histidine	-0.502	0.02211
Lysine	-1.225	0.00667
Proline	-0.619	0.03764
Threonine	-0.960	0.20107
Valine	-0.892	0.00397

S1 DL-Alanine Hygroscopicity

Fig. S1.1: Hygroscopicity of DL-Alanine (Sigma Aldrich, Purity 99 %) at 293.15 K.

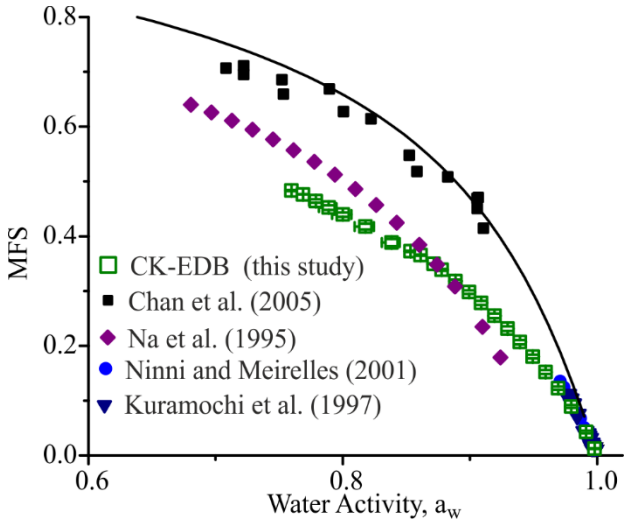

Table S1.1: Pure component refractive index (n_{melt}) is determined using molar refraction, assuming ideal mixing for calculation of the melt density (ρ_{melt}), from bulk data available in Cai et al. (2016). The variation of density as a function of the root of solute mass fraction ($MFS^{1/2} = x$) is represented by polynomial fit parameters. *Upper* and *lower* refer to 95 % confidence limits for fits to experimental data, (Section 2.2 in manuscript).

			Polynomial fit ($\rho_{sol} = a + b_1x + b_2x^2 + b_3x^3$)			
	n_{melt}	ρ_{melt}/ g.cm^{-3}	a	b_1	b_2	b_3
Best	1.6205	1.4961	999	94.14	-66.93	466.48
Upper	1.6222	1.5042	999	97.38	-76.61	480.88
Lower	1.6188	1.4881	999	90.98	-57.61	452.44

Table S1.2: Tabulated experimental data points shown in **Fig S1.1.**

a_w	error a_w (+ve)	error a_w (-ve)	MFS	error MFS
0.75966	0.00182	0.00228	0.48336	8.66E-04
0.76866	1.02E-03	0.00128	0.47642	3.48E-04
0.77876	0.00413	0.00519	0.46428	0.00314
0.78887	0.00613	0.00771	0.45228	0.00412
0.80001	0.00674	0.00847	0.43959	0.00395
0.81774	0.00674	8.47E-03	0.41748	0.00512
0.83836	6.17E-03	7.75E-03	0.38848	6.39E-03
0.85334	0.00473	3.00E-03	0.37246	0.00116
0.86108	0.00116	7.54E-04	0.3655	8.92E-04
0.87144	6.02E-04	4.18E-04	0.34973	5.50E-04
0.87774	0.00139	9.81E-04	0.3386	0.00165
0.88866	0.00217	0.00153	0.31805	0.00274
0.89931	2.66E-03	1.92E-03	0.2981	0.00333
0.9087	0.00257	0.00183	0.27841	0.00381
0.91923	0.00256	0.00191	0.25483	0.00426
0.92957	0.00248	0.00181	0.23142	0.00416
0.93936	0.00243	0.00179	0.20672	0.00392
0.94936	0.00206	1.54E-03	0.18027	0.00361
0.9595	1.95E-03	1.43E-03	0.15211	0.00347
0.96935	1.49E-03	1.11E-03	0.12252	0.003
0.97954	0.00127	9.28E-04	0.08929	0.00254
0.99143	6.34E-04	7.22E-04	0.04259	0.00238

S2 L-Arginine Hygroscopicity

Fig S2.1: Hygroscopicity of L-Arginine, (Acros Organics, Purity > 98 %), at 293.15 K. Open squares, these experiments.

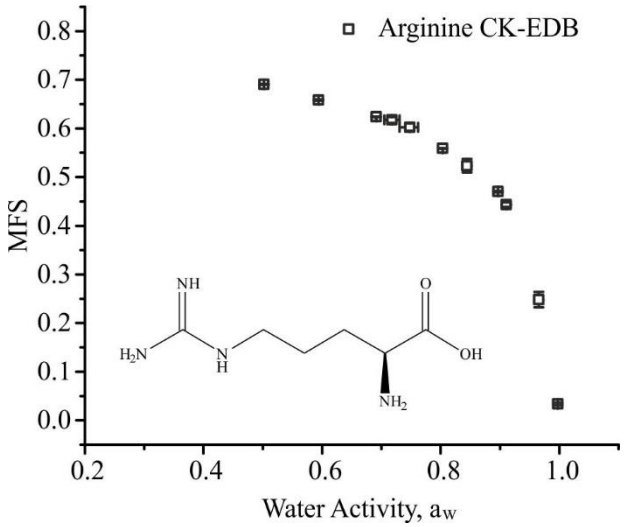

Table S2.1: Pure component refractive index (n_{melt}) is determined using molar refraction, assuming ideal mixing for calculation of the melt density (ρ_{melt}), from bulk data available in Cai et al. (2016). The variation of density as a function of the root of solute mass fraction (MFS $^{1/2}$ =x) is represented by polynomial fit parameters. *Upper* and *lower* refer to 95 % confidence limits for fits to experimental data, (Section 2.2 in manuscript).

			Polynomial fit ($\rho_{sol} = a + b_1x + b_2x^2 + b_3x^3$)			
	n_{melt}	ρ_{melt}/ g.cm^{-3}	a	b_1	b_2	b_3
Best	1.637	1.3995	998.6	59.85	28.54	310.48
Upper	1.6382	1.4045	998.6	61.44	24.47	317.9
Lower	1.6358	1.3945	998.6	58.28	32.51	303.13

Table S2.2: Tabulated experimental data points shown in **Fig S2.1.**

a_w	error a_w (+ve)	error a_w (-ve)	MFS	error MFS
0.50205	0.00177	0.0021	0.69041	0.00113
0.59399	0.00171	0.00206	0.65822	0.00115
0.69132	0.00127	0.00157	0.62391	1.74E-04
0.71788	0.01297	0.01296	0.61768	0.00607
0.74796	0.0139	0.01716	0.6026	0.00755
0.80315	7.87E-04	0.001	0.55889	4.50E-04
0.84439	0.00739	0.00741	0.52351	0.014
0.89694	0.00128	0.00112	0.47038	0.00138
0.91074	0.00174	0.00175	0.44361	0.00473
0.96538	0.00317	0.00317	0.24814	0.01569
0.99761	5.53E-04	5.28E-04	0.03416	0.00266

S3 Glycine Hygroscopicity

Fig S3.1: Hygroscopicity of Glycine, (Santa Cruz Biotech LTD), at 293.15 K. Solid line standard UNIFAC prediction.

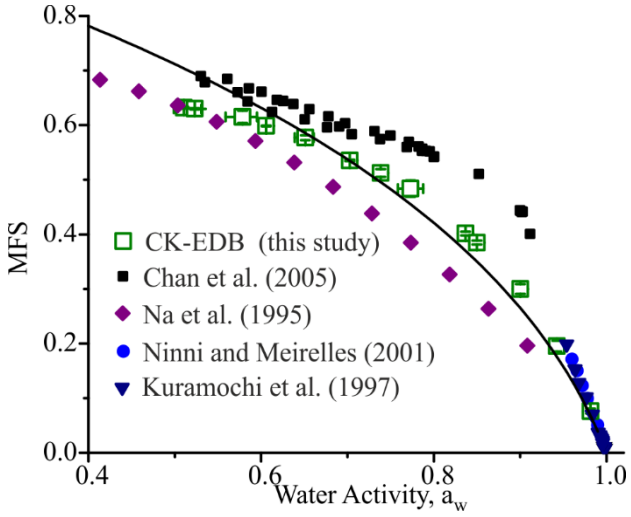

Table S3.1: Pure component refractive index (n_{melt}) is determined using molar refraction, assuming ideal mixing for calculation of the melt density (ρ_{melt}), from bulk data available in Cai et al. (2016). The variation of density as a function of the root of solute mass fraction (MFS $^{1/2}$ =x) is represented by polynomial fit parameters. *Upper* and *lower* refer to 95 % confidence limits for fits to experimental data, (Section 2.2 in manuscript).

			Polynomial fit ($\rho_{sol} = a + b_1x + b_2x^2 + b_3x^3$)			
	n_{melt}	ρ_{melt}/ $g.cm^{-3}$	a	b_1	b_2	b_3
Best	1.6634	1.6905	999.47	186.75	-363.66	860.4
Upper	1.6654	1.7006	999.47	192.41	-382.69	883.61
Lower	1.6613	1.6805	999.47	181.22	-345.14	837.67

Table S3.2: Tabulated experimental data points shown in **Fig S3.1.**

a_w	error a_w (+ve)	error a_w (-ve)	MFS	error MFS
0.51061	0.00328	0.00389	0.63189	0.00159
0.52315	0.0204	0.02421	0.62993	0.00129
0.57855	0.01673	0.01985	0.61512	0.01113
0.60598	0.00228	0.00276	0.59862	6.15E-04
0.65105	0.00995	0.01205	0.57691	0.00441
0.70256	0.00157	0.00195	0.53551	0.00146
0.73844	0.0068	0.00678	0.51233	0.00686
0.77309	0.01453	0.01453	0.48382	0.01515
0.83663	0.0021	0.00115	0.4015	0.00347
0.84998	0.00206	0.00204	0.38496	0.00336
0.90029	0.00391	0.00391	0.29984	0.00906
0.94266	0.00341	0.00339	0.19519	0.00966
0.98152	0.00147	0.00147	0.07624	0.00455

S4 Histidine Hygroscopicity

Fig S4.1: Hygroscopicity of L-Histidine, (VWR Chemicals), open symbols, these CC-EDB experiments.

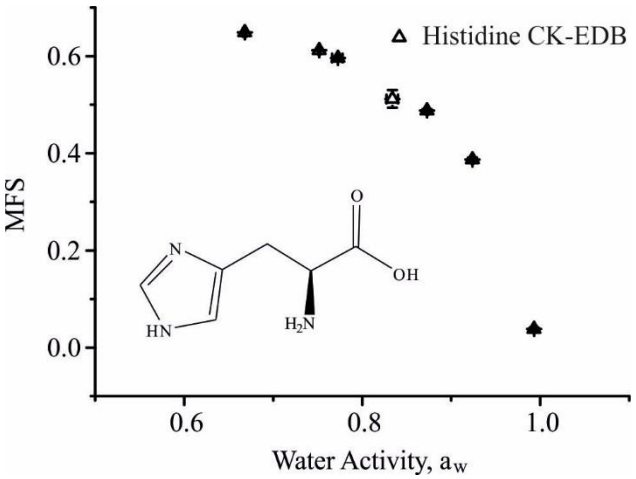

Table S4.1: Pure component refractive index (n_{melt}) is determined using molar refraction, assuming ideal mixing for calculation of the melt density (ρ_{melt}), from bulk data available in Cai et al. (2016). The variation of density as a function of the root of solute mass fraction (MFS $^{1/2}$ =x) is represented by polynomial fit parameters. *Upper* and *lower* refer to 95 % confidence limits for fits to experimental data, (Section 2.2 in manuscript).

			Polynomial fit ($\rho_{sol} = a + b_1x + b_2x^2 + b_3x^3$)			
	n_{melt}	ρ_{melt}/ $g.cm^{-3}$	a	b_1	b_2	b_3
Best	1.6892	1.5378	998.9	111.5	-119.61	542.86
Upper	1.6914	1.5462	998.9	115.17	-130.97	558.8
Lower	1.6871	1.5296	998.9	107.98	-108.77	527.49

Table S4.2: Tabulated experimental data points shown in **Fig S4.1.**

a_w	error a_w (+ve)	error a_w (-ve)	MFS	error MFS
		293.15 K		
0.66801	0.00175	0.00214	0.64888	5.85836E-4
0.75174	0.00105	0.00131	0.61182	3.82887E-4
0.77265	0.00527	0.00661	0.59614	0.00177
0.83375	0.0064	0.00643	0.51198	0.01825
0.87281	0.00111	0.00101	0.48826	0.0027
0.9239	8.9548E-4	9.46372E-4	0.38721	0.00439
0.99296	6.37951E-4	6.3374E-4	0.03829	0.00295

S5 L-Lysine Hygroscopicity

Fig S5.1: Hygroscopicity of L-Lysine, (Sigma Aldrich, Purity ≥ 98 %), at 293.15 K. Open squares, these experiments; solid line, UNIFAC model.

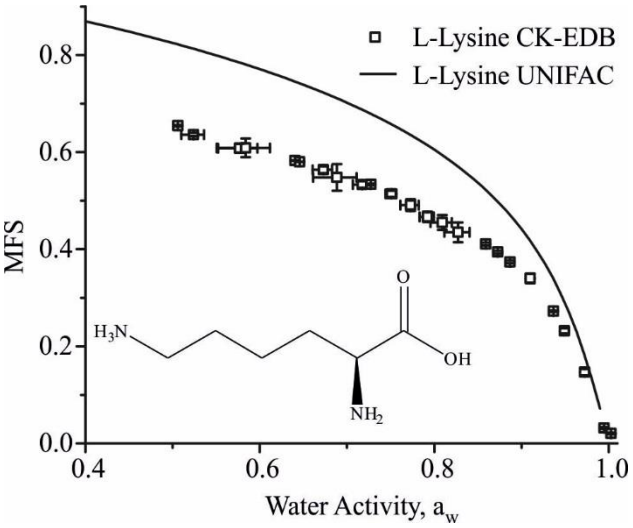

Table S5.1: Pure component refractive index (n_{melt}) determined using molar refraction where the melt density (ρ_{melt}), is determined using a polynomial fit of density to the square root of MFS ($MFS^{1/2}$ =x). Bulk values used are available in Cai et al. (2016). *Upper* and *lower* refer to 95 % confidence limits for fits to experimental data.

			Polynomial fit ($\rho_{sol} = a + b_1x + b_2x^2 + b_3x^3$)			
	n_{melt}	ρ_{melt}/ $g.cm^{-3}$	a	b_1	b_2	b_3
Best	1.5586	1.2362	998.2	-15.22	309.14	-56.02
Upper	1.5614	1.2418	998.2	-4.29	271.92	-23.99
Lower	1.5558	1.2306	998.2	-25.93	346.35	-88.05

Table S5.2: Tabulated experimental data points shown in **Fig S5.1.**

a_w	error a_w (+ve)	error a_w (-ve)	MFS	error MFS
0.50605	0.00267	0.00316	0.65479	0.00157
0.52404	0.01187	0.01406	0.63621	0.00337
0.57666	0.02059	0.02439	0.60815	0.00948
0.58372	0.02793	0.03308	0.60867	0.01931
0.64049	0.00405	0.00494	0.58275	4.04084E-4
0.64559	0.00205	0.00251	0.57997	4.926E-4
0.67292	0.00999	0.0122	0.56365	0.00675
0.68839	0.0225	0.02735	0.54807	0.02742
0.71755	0.00885	0.01092	0.53328	0.00647
0.72732	0.00179	0.00223	0.53359	0.00179
0.75098	0.0056	0.00696	0.51408	0.00626
0.77291	0.00939	0.01164	0.49095	0.01194
0.79224	0.00736	0.00909	0.46681	0.01099
0.80926	0.01092	0.01352	0.45505	0.01535
0.82751	0.01292	0.01604	0.43489	0.02026
0.85916	0.00152	0.00197	0.41093	0.00309
0.87288	0.00143	0.00143	0.39407	0.00288
0.88688	0.00151	0.00151	0.3739	0.00294
0.90999	0.00294	0.00337	0.33998	0.00983
0.93683	3.20551E-4	3.24824E-4	0.27222	0.00154
0.94931	0.00162	0.00162	0.23179	0.00544
0.97255	0.00147	0.00147	0.14683	0.00623
0.99465	4.49456E-4	4.50168E-4	0.03174	0.0021
1.00277	0.00113	0.00149	0.02039	0.00198

S6 L-Proline Hygroscopicity

Figure S6.1: Hygroscopicity of L-Proline, (Acros Organics, Purity + 99 %), at 293.15 K. Open squares, these experiments.

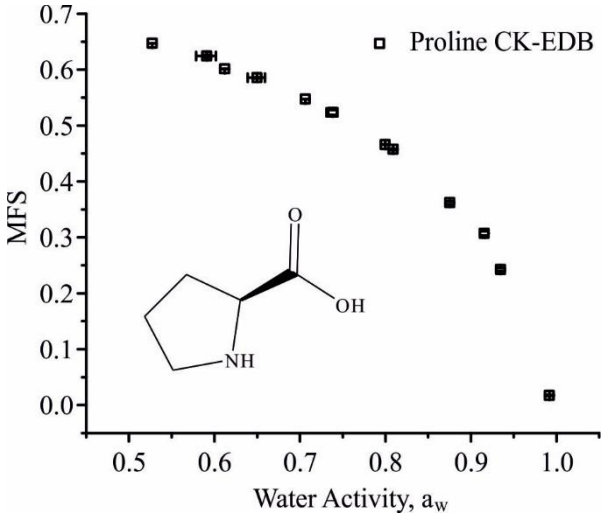

Table S6.1: Pure component refractive index (n_{melt}) is determined using molar refraction, assuming ideal mixing for calculation of the melt density (ρ_{melt}), from bulk data available in Cai et al. (2016). The variation of density as a function of the root of solute mass fraction (MFS $^{1/2}$ =x) is represented by polynomial fit parameters. *Upper* and *lower* refer to 95 % confidence limits for fits to experimental data, (Section 2.2 in manuscript).

			Polynomial fit ($\rho_{sol} = a + b_1x + b_2x^2 + b_3x^3$)			
	n_{melt}	ρ_{melt}/ $g.cm^{-3}$	a	b_1	b_2	b_3
Best	1.5948	1.3866	999	55.7	39.01	291
Upper	1.5964	1.3945	999	58.13	32.96	302.44
Lower	1.5932	1.3788	999	53.36	44.73	279.93

Table S6.2: Tabulated experimental data points shown in **Fig S6.1.**

a_w	error a_w (+ve)	error a_w (-ve)	MFS	error MFS
0.52739	0.00183	0.00218	0.647	1.53E-04
0.59111	0.01061	0.01264	0.62414	0.00218
0.61213	0.00154	0.00186	0.6013	1.44E-04
0.64995	0.00905	0.01098	0.58549	0.00122
0.70619	9.52E-04	0.00118	0.54716	3.08E-04
0.73823	0.0057	0.00705	0.52349	0.00436
0.79982	7.99E-04	0.00101	0.46617	7.45E-04
0.80883	0.00112	0.00112	0.45742	1.45E-03
0.87515	1.30E-03	0.00103	0.36217	2.56E-03
0.91551	0.00145	0.00184	0.30701	0.00352
0.93455	9.07E-04	9.29E-04	0.24258	0.00279
0.99172	5.01E-04	5.60E-04	0.01734	0.0011

S7 L-Threonine Hygroscopicity

Fig S7.1: Hygroscopicity of L-Threonine, (Acros Organics, Purity 98 %), at 293.15 K. Open squares, these experiments; solid line, UNIFAC model.

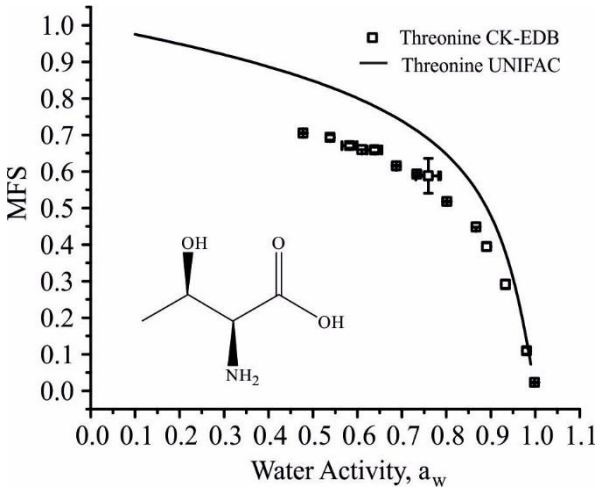

Table S7.1: Pure component refractive index (n_{melt}) is determined using molar refraction, assuming ideal mixing for calculation of the melt density (ρ_{melt}), from bulk data available in Cai et al. (2016). The variation of density as a function of the root of solute mass fraction ($MFS^{1/2} = x$) is represented by polynomial fit parameters. *Upper* and *lower* refer to 95 % confidence limits for fits to experimental data, (Section 2.2 in manuscript).

			Polynomial fit ($\rho_{sol} = a + b_1x + b_2x^2 + b_3x^3$)			
	n_{melt}	ρ_{melt}/ $g.cm^{-3}$	a	b_1	b_2	b_3
Best	1.6185	1.4977	999.4	94.57	-68.14	468.44
Upper	1.6274	1.5403	999.4	112.31	-121.99	546.4
Lower	1.6102	1.4575	999.4	79.24	-23.63	399.69

Table S7.2: Tabulated experimental data points shown in **Fig S7.1.**

a_w	error a_w (+ve)	error a_w (-ve)	MFS	error MFS
0.47807	0.00212	0.0025	0.70511	0.00173
0.53888	0.0052	0.0062	0.69319	0.00723
0.58237	0.01442	0.01711	0.67043	0.00714
0.60978	0.00127	0.00154	0.65941	3.88E-04
0.63867	0.01393	0.01689	0.65875	0.00707
0.68779	0.00158	0.00195	0.61529	0.00161
0.73352	0.0081	0.00812	0.59255	0.0041
0.75945	0.02291	0.02781	0.58815	0.04754
0.80118	0.00157	7.31E-04	0.51778	0.00135
0.86674	7.26E-04	4.84E-04	0.44784	3.66E-04
0.89045	0.00426	0.00419	0.39429	0.0104
0.93289	0.00438	0.00418	0.29104	0.01212
0.98064	0.00213	0.00214	0.10966	0.00862
0.99865	7.16E-04	4.45E-04	0.02317	0.00125

S8 L-Valine Hygroscopicity

Figure S8.1: Hygroscopicity of L-Valine, (Sigma Aldrich, Purity ≥ 98 %), at 293.15 K (blue Open symbols, these CK-EDB experiments; black filled circles, literature data (Kuramochi *et al.*); solid black line, UNIFAC model (293.15 K).

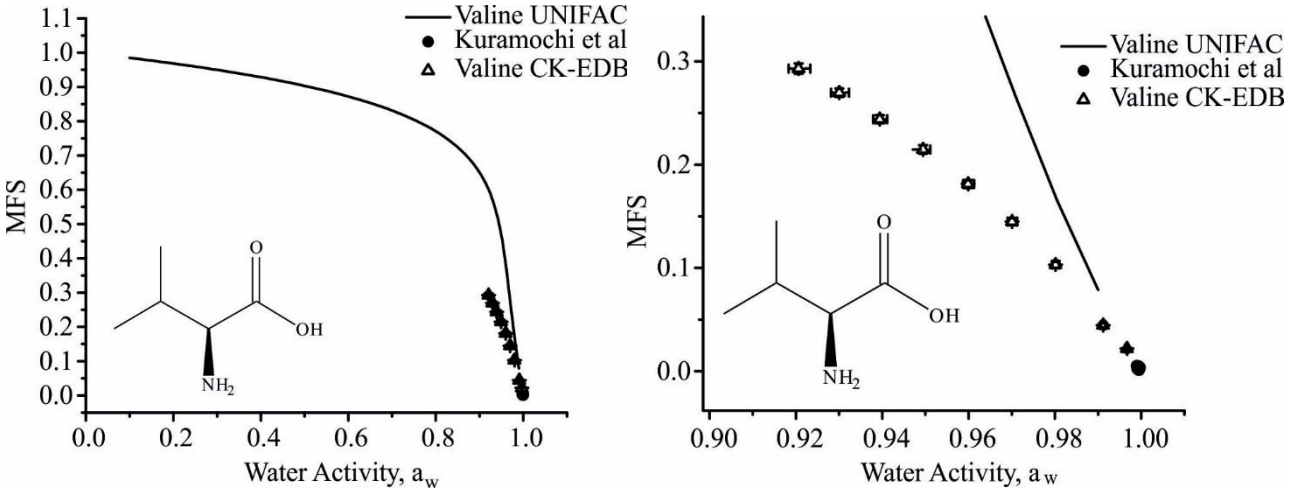

Table S8.1: Pure component refractive index (n_{melt}) is determined using molar refraction, assuming ideal mixing for calculation of the melt density (ρ_{melt}), from bulk data available in Cai et al. (2016). The variation of density as a function of the root of solute mass fraction ($MFS^{1/2} = x$) is represented by polynomial fit parameters. *Upper* and *lower* refer to 95 % confidence limits for fits to experimental data, (Section 2.2 in manuscript).

			Polynomial fit ($\rho_{sol} = a + b_1x + b_2x^2 + b_3x^3$)			
	n_{melt}	ρ_{melt}/ $g.cm^{-3}$	a	b_1	b_2	b_3
Best	1.5791	1.2824	998.77	28.73	94.37	159.64
Upper	1.58	1.2872	998.77	29.8	92.82	164.91
Lower	1.5781	1.2776	998.77	27.71	95.81	154.45

Table S8.2: Tabulated experimental data points shown in **Fig S8.1.**

a_w	error a_w (+ve)	error a_w (-ve)	MFS	error MFS
		293.15 K		
0.92062	0.0027	0.00232	0.29295	0.00499
0.93004	2.26E-03	0.00195	0.26962	4.18E-03
0.93941	0.00173	0.00148	0.24396	0.00404
0.94943	0.00169	0.00145	0.21478	0.00403
0.9599	0.00138	0.00118	0.18125	0.00388
0.97008	0.00118	0.00101	0.14482	0.00345
0.98014	8.66E-04	7.41E-04	0.10314	2.94E-03
0.99117	5.34E-04	5.69E-04	0.04451	0.00201
0.99669	4.13E-04	4.57E-04	0.02205	8.65E-04

S9 Citric Acid Hygroscopicity

Figure S9.1: Hygroscopicity of Citric Acid, (Sigma Aldrich, Purity 99 %), at 293.15 K. Open squares, these EDB experiments; solid line, UNIFAC model.

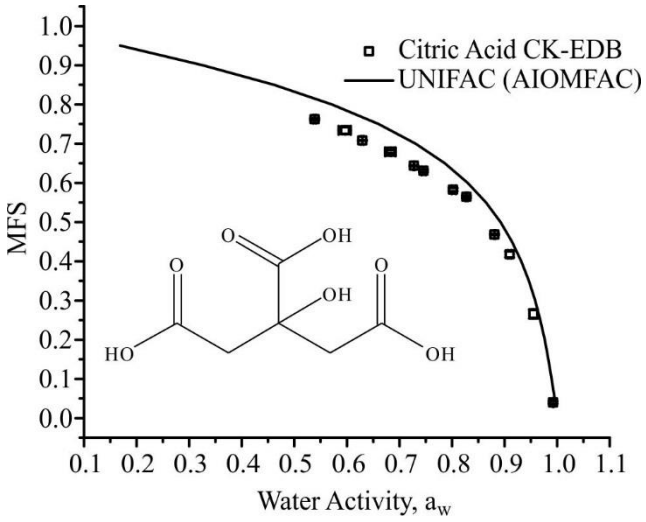

Table S9.1: Pure component refractive index (n_{melt}) determined using molar refraction where the melt density (ρ_{melt}) is determined using a polynomial fit of density to the square root of MFS ($MFS^{½} = x$). Bulk values used are available in Cai et al. (2016). *Upper* and *lower* refer to 95 % confidence limits for fits to experimental data.

			Polynomial fit ($\rho_{sol} = a + b_1x + b_2x^2 + b_3x^3$)			
	n_{melt}	ρ_{melt}/ $g.cm^{-3}$	a	b_1	b_2	b_3
Best	1.5054	1.550	998.0	25.0	253.84	273.2
Upper	1.5071	1.5565	998.0	37.88	211.13	309.49
Lower	1.5037	1.5436	998.0	12.11	296.56	236.92

Table S9.2: Tabulated experimental data points shown in **Fig S9.1.**

a_w	error a_w (+ve)	error a_w (-ve)	MFS	error MFS
0.53894	0.0024	0.00286	0.76226	0.00233
0.59688	0.01043	0.01244	0.73375	0.00875
0.62961	0.00223	0.00271	0.70793	7.62E-04
0.6837	0.00876	0.01065	0.67914	0.00409
0.72762	0.00123	0.00153	0.64368	0.00135
0.74592	0.00403	0.00404	0.63069	0.00342
0.80229	0.00504	0.0029	0.58246	0.00401
0.82734	0.00237	0.00196	0.56406	0.00314
0.88104	0.00107	0.0012	0.4682	0.00149
0.90968	0.00331	0.00327	0.41761	0.00738
0.95487	0.0028	0.00279	0.26562	0.01165
0.99255	6.21E-04	6.70E-04	0.03973	0.00355

S10 L-Tartaric Acid Hygroscopicity

Figure S10.1: Hygroscopicity of Tartaric Acid, (Sigma Aldrich, Purity ≥ 99.5 %), at 293.15 K. Open squares, these EDB experiments; solid line, UNIFAC model.

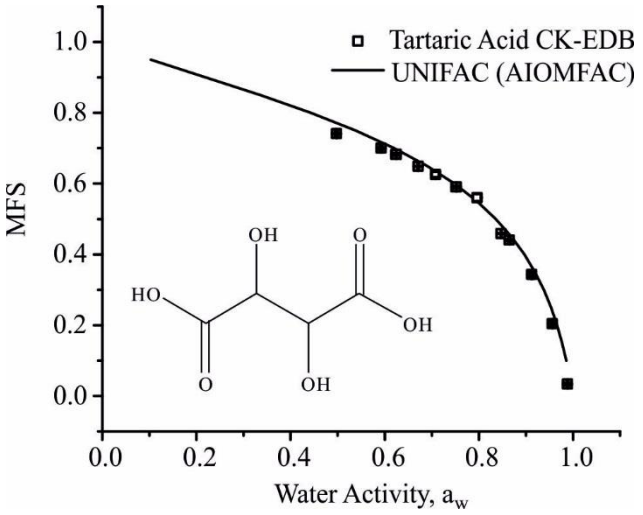

Table S10.1: Pure component refractive index (n_{melt}) determined using molar refraction where the melt density (ρ_{melt}) is determined using a polynomial fit of density to the square root of MFS ($MFS^{½} = x$). Bulk values used are available in Cai et al. (2016). *Upper* and *lower* refer to 95 % confidence limits for fits to experimental data.

			Polynomial fit ($\rho_{sol} = a + b_1x + b_2x^2 + b_3x^3$)			
	n_{melt}	ρ_{melt}/ g.cm^{-3}	a	b_1	b_2	b_3
Best	1.4992	1.6007	999	15.08	325.84	260.78
Upper	1.4996	1.6128	999	29.23	273.11	311.49
Lower	1.4936	1.5886	999	93.2	378.58	210.06

Table S10.2: Tabulated experimental data points shown in **Fig S10.1.**

a_w	error a_w (+ve)	error a_w (-ve)	MFS	error MFS
0.49764	0.00285	0.00337	0.74075	0.00145
0.59229	0.00275	0.00332	0.70005	0.00184
0.62457	0.00897	0.01082	0.68273	0.00361
0.67107	0.00165	0.00203	0.64893	7.95E-04
0.70799	0.00711	0.00826	0.6255	0.0076
0.75229	0.00853	0.01048	0.59046	0.00337
0.79666	0.00778	0.00946	0.56049	0.00992
0.84739	9.37E-04	5.51E-04	0.45906	0.00122
0.86463	0.00206	0.00206	0.44068	0.00269
0.91248	0.00302	0.00302	0.34362	0.00774
0.95599	0.00217	0.00216	0.20415	0.00789
0.98847	0.00104	0.00105	0.03363	0.00337

S11 Oxalic Acid Hygroscopicity

Fig S11.1: Hygroscopicity of Oxalic Acid, (Sigma Aldrich, Purity 98 %), at 293.15 K. Open squares, these experiments; solid line, UNIFAC model.

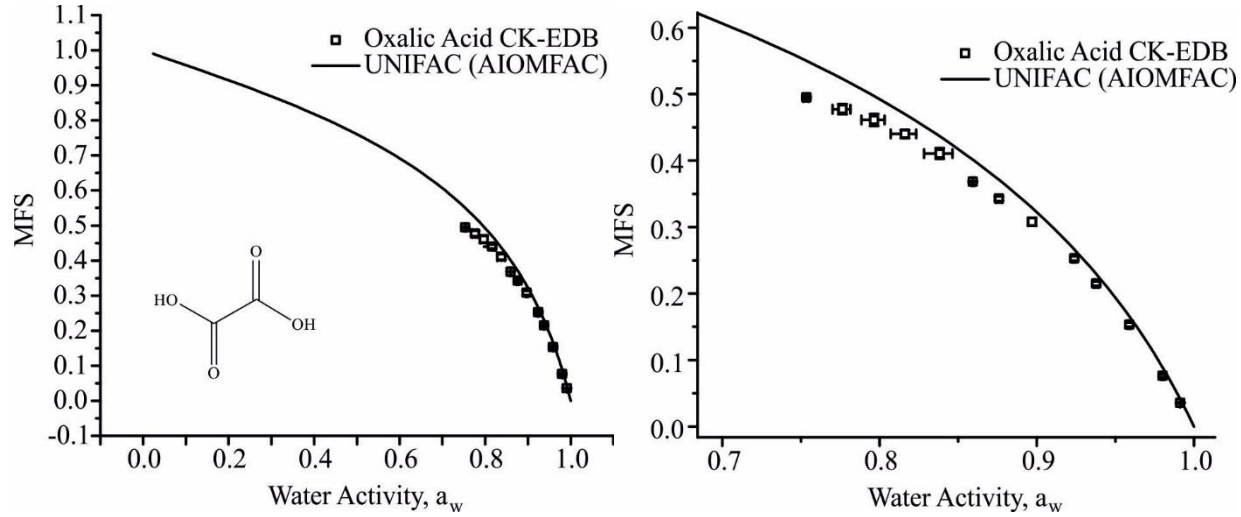

Table S11.1: Pure component refractive index (n_{melt}) is determined using molar refraction, assuming ideal mixing for calculation of the melt density (ρ_{melt}), from bulk data available in Cai et al. (2016). The variation of density as a function of the root of solute mass fraction ($MFS^{1/2}$ =x) is represented by polynomial fit parameters. *Upper* and *lower* refer to 95 % confidence limits for fits to experimental data, (Section 2.2 in manuscript).

			Polynomial fit ($\rho_{sol} = a + b_1x + b_2x^2 + b_3x^3 + b_4x^4 + b_5x^5 + b_6x^6$)						
	n_{melt}	ρ_{melt}/ $g.cm^{-3}$	a	b_1	b_2	b_3	b_4	b_5	b_6
Best	1.5167	1.7237	998.4	-14.98	636.47	-1074.2	2603.92	-2596.5	1170.54
Upper	1.5185	1.7403	998.4	-16.27	660.48	-1165.1	2811.06	-2809	1260.66
Lower	1.5149	1.7073	998.4	-13.78	613.65	-989.39	2409.96	-2397.5	1085.84

Table S11.2: Tabulated experimental data points shown in **Fig S11.1.**

a_w	error a_w (+ve)	error a_w (-ve)	MFS	error MFS
0.75352	0.00146	0.00183	0.49497	0.00148
0.77652	0.00502	0.00629	0.47731	0.0077
0.79664	0.00652	0.00817	0.46116	0.00912
0.81614	0.00716	0.00896	0.44009	0.00613
0.83841	0.00803	0.01005	0.41068	0.00808
0.85938	0.0012	7.60E-04	0.36829	0.00113
0.87602	0.00199	0.00188	0.34275	0.00355
0.89702	0.00235	0.00215	0.30804	0.00596
0.92388	8.50E-04	0.00115	0.25275	0.00331
0.93784	0.00106	0.00106	0.21515	0.00299
0.9589	8.73E-04	8.75E-04	0.15314	0.00313
0.98012	5.72E-04	5.68E-04	0.07645	0.00227
0.99129	2.93E-04	3.54E-04	0.03567	8.98E-04

S12 Malonic Acid Hygroscopicity

Figure S12.1: Hygroscopicity of Malonic Acid, (Sigma Aldrich, Purity 98 %), at 293.15 K. Open squares, these experiments; solid line, UNIFAC model.

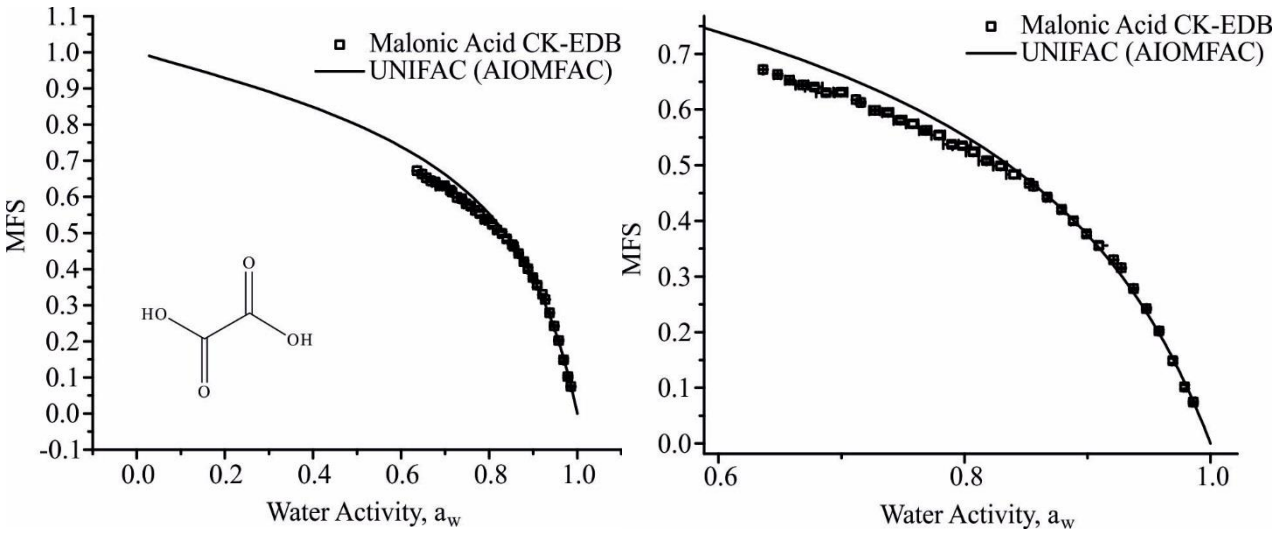

Table S12.1: Pure component refractive index determined using molar refraction where the melt density is determined using a polynomial fit of density to the square root of MFS ($MFS^{1/2}$ =x). Bulk values used are available in Cai et al. (2016). *Upper* and *lower* refer to 95 % confidence limits for fits to experimental data.

			Polynomial fit ($\rho_{sol} = a + b_1x + b_2x^2 + b_3x^3$)			
	n_{melt}	ρ_{melt}/ $g.cm^{-3}$	a	b_1	b_2	b_3
Best	1.4611	1.4558	997.2	13.47	262.36	182.76
Upper	1.4627	1.4612	997.2	20.7	235.91	207.37
Lower	1.4594	1.4504	997.2	6.24	288.82	158.15

Table S12.2: Tabulated experimental data points shown in **Fig S12.1.**

a_w	error a_w (+ve)	error a_w (-ve)	MFS	error MFS
0.63613	4.14E-04	5.04E-04	0.6718	1.62E-04
0.64803	0.00253	0.00308	0.66275	0.00161
0.65776	0.00301	0.00367	0.65273	0.00197
0.66822	0.00457	0.00558	0.64421	0.00162
0.67795	0.00624	0.00761	0.64043	0.00324
0.68747	0.00679	0.00828	0.62992	0.00337
0.6994	0.0051	0.00625	0.63085	0.00413
0.7117	4.61E-04	5.72E-04	0.6176	2.85E-04
0.71572	0.00132	0.00164	0.61275	0.00135
0.72728	0.00371	0.00458	0.59849	0.00119
0.73786	0.00398	0.0049	0.59485	0.00362
0.74792	0.00441	0.00544	0.58075	0.00309
0.75777	0.00438	0.00539	0.57442	0.00518
0.76852	0.00437	0.00539	0.56217	0.00227
0.77901	0.00483	0.00595	0.55399	0.00568
0.78948	0.00564	0.00694	0.53743	0.0039
0.79831	0.00665	0.00816	0.53501	0.00406
0.80703	0.00469	0.00576	0.52388	0.00468
0.81779	0.00517	0.00637	0.50809	0.00307
0.82931	0.00495	0.0061	0.49855	0.00449
0.83997	0.00501	0.00616	0.48341	0.0058
0.85259	0.0013	8.20E-04	0.46721	9.32E-04
0.85596	0.00112	6.98E-04	0.46233	0.00114
0.86726	0.00223	0.00146	0.44257	0.00286
0.87898	0.00278	0.00183	0.4203	0.0033
0.8885	0.00291	0.00204	0.4002	0.0044

0.89906	0.00294	0.00205	0.37643	0.00371
0.90919	0.00337	0.00233	0.35563	0.00559
0.9213	1.65E-04	2.03E-04	0.32987	3.33E-04
0.92743	2.61E-04	2.85E-04	0.31545	0.00122
0.93737	3.90E-04	4.01E-04	0.27835	0.00185
0.94793	4.69E-04	4.71E-04	0.24233	0.00205
0.95802	4.67E-04	4.69E-04	0.20227	0.00223
0.96932	0.0018	0.0011	0.14857	0.00427
0.97897	0.00144	8.79E-04	0.10171	0.00358
0.98599	0.00158	9.62E-04	0.07431	0.00205

S13 Succinic Acid Hygroscopicity

Fig S13.1: Hygroscopicity of Succinic Acid, (Sigma Aldrich, Purity 99 %), at 293.15 K. Open squares, these experiments; solid line, UNIFAC model.

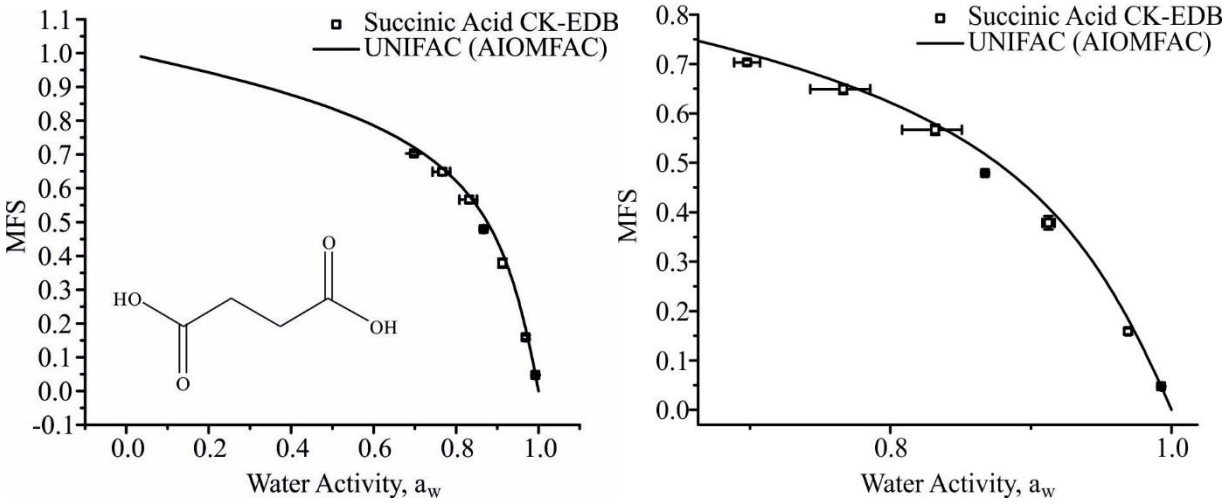

Table S13.1: Pure component refractive index (n_{melt}) is determined using molar refraction, assuming ideal mixing for calculation of the melt density (ρ_{melt}), from bulk data available in Cai et al. (2016). The variation of density as a function of the root of solute mass fraction ($MFS^{1/2} = x$) is represented by polynomial fit parameters. *Upper* and *lower* refer to 95 % confidence limits for fits to experimental data, (Section 2.2 in manuscript).

			Polynomial fit ($\rho_{sol} = a + b_1x + b_2x^2 + b_3x^3 + b_4x^4 + b_5x^5 + b_6x^6$)						
	n_{melt}	ρ_{melt}/ g.cm^{-3}	a	b_1	b_2	b_3	b_4	b_5	b_6
Best	1.4928	1.4185	998.2	-1.96	324.69	-146.48	426.3	-373.62	191.37
Upper	1.4935	1.4249	998.2	-2.08	329.57	-155.12	447.91	-395.04	201.45
Lower	1.4920	1.4122	998.2	-1.85	319.93	-138.32	405.79	-353.36	181.79

Table S13.2: Tabulated experimental data points shown in **Fig S13.1.**

a_w	error a_w (+ve)	error a_w (-ve)	MFS	error MFS
0.69803	0.00919	0.00918	0.70299	0.00502
0.76653	0.0191	0.02355	0.64896	0.00963
0.83176	0.0191	0.02355	0.56672	0.01018
0.86728	0.00142	0.00142	0.47926	0.0025
0.91247	0.00444	0.0044	0.37868	0.01328
0.96915	0.00137	0.00136	0.15909	0.00637
0.99255	3.09E-04	3.16E-04	0.04733	0.00178

S14 Glutaric Acid Hygroscopicity

Figure S14.1: Hygroscopicity of Glutaric Acid, (Sigma Aldrich, Purity 99 %), at 293.15 K. Open squares, these experiments; solid line, UNIFAC model.

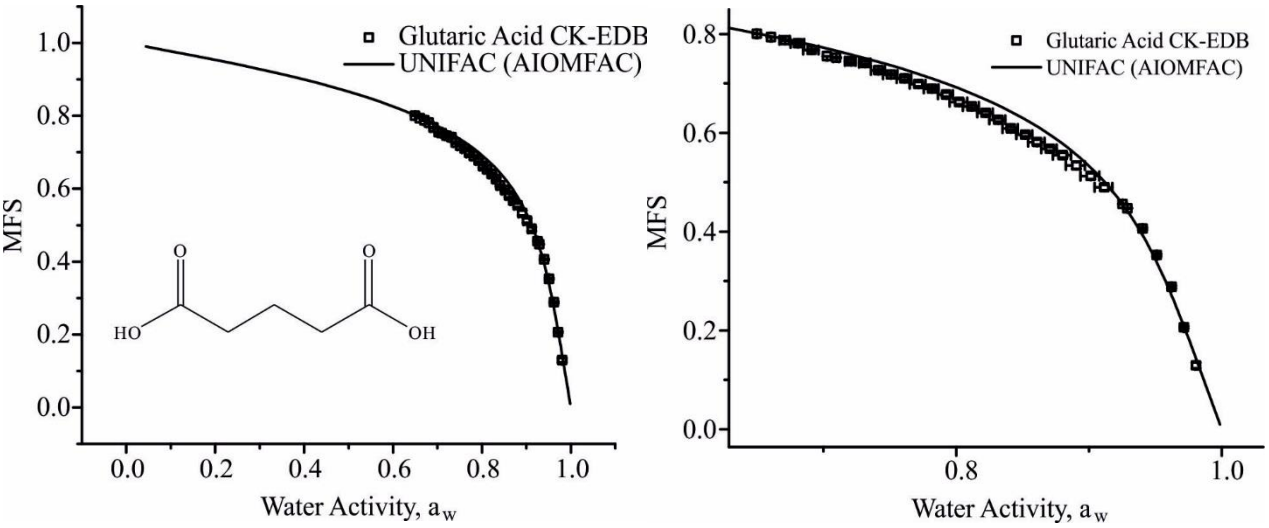

Table S14.1: Pure component refractive index (n_{melt}) determined using molar refraction where the melt density (ρ_{melt}) is determined using a polynomial fit of density to the square root of MFS ($MFS^{1/2}$ =x). Bulk values used are available in Cai et al. (2016). *Upper* and *lower* refer to 95 % confidence limits for fits to experimental data.

			Polynomial fit ($\rho_{sol} = a + b_1x + b_2x^2 + b_3x^3$)			
	n_{melt}	ρ_{melt}/ $g.cm^{-3}$	a	b_1	b_2	b_3
Best	1.4655	1.2745	997.5	-1.56	238.79	39.75
Upper	1.4660	1.2760	997.5	0.401	231.59	46.55
Lower	1.4649	1.2729	997.5	-3.53	245.98	32.95

Table S14.2: Tabulated experimental data points shown in **Fig S14.1.**

a_w	error a_w (+ve)	error a_w (-ve)	MFS	error MFS
0.64988	4.93E-04	6.03E-04	0.80052	2.01E-04
0.66053	5.88E-04	7.21E-04	0.79339	2.71E-04
0.67122	0.00348	0.00426	0.78724	9.92E-04
0.68089	0.00458	0.00561	0.78134	0.00256
0.69112	0.00522	0.00639	0.76761	0.00226
0.70268	4.02E-04	4.98E-04	0.75519	1.75E-04
0.70969	0.0019	0.00235	0.75207	8.79E-04
0.72069	0.00357	0.00441	0.74499	0.00276
0.73156	0.0038	0.00469	0.74131	0.003
0.74152	0.00467	0.00575	0.72636	0.00217
0.75089	0.00485	0.00598	0.71793	0.00185
0.76119	0.00482	0.00594	0.70997	0.00323
0.77157	0.00535	0.00659	0.69846	0.00478
0.7818	0.00495	0.0061	0.68945	0.00241
0.79242	0.00502	0.00618	0.6775	0.00399
0.80236	5.99E-03	7.39E-03	0.6624	0.00435
0.81173	5.37E-03	6.62E-03	0.65327	0.00271
0.82228	0.00521	0.00642	0.64016	0.00336
0.83171	0.00538	0.00662	0.62617	0.00336
0.84134	0.00521	0.00642	0.60886	0.0028
0.852	0.00538	0.00663	0.59616	0.00364
0.86106	0.00556	0.00684	0.58136	0.00487
0.87055	0.00521	0.00642	0.56748	0.00361
0.88031	0.00617	0.00761	0.5545	0.00465
0.89058	0.00635	0.00785	0.5337	0.00679
0.90142	0.00628	0.00777	0.51244	0.00601

0.91173	0.00596	0.00737	0.48949	0.00523
0.92543	1.50E-04	2.02E-04	0.45608	4.73E-04
0.92905	1.56E-04	1.58E-04	0.44732	6.46E-04
0.94053	3.86E-04	3.86E-04	0.40605	0.00233
0.95111	4.52E-04	4.52E-04	0.35279	0.00256
0.96227	3.42E-04	3.41E-04	0.28818	0.00275
0.97153	3.20E-04	3.20E-04	0.20634	0.00243
0.98066	8.31E-04	8.09E-04	0.12936	0.00558

S15 Adipic Acid Hygroscopicity

Figure S15.1: Hygroscopicity of Adipic Acid, (Sigma Aldrich, Purity 99 %), at 293.15 K. Open squares, these experiments; solid line, UNIFAC model.

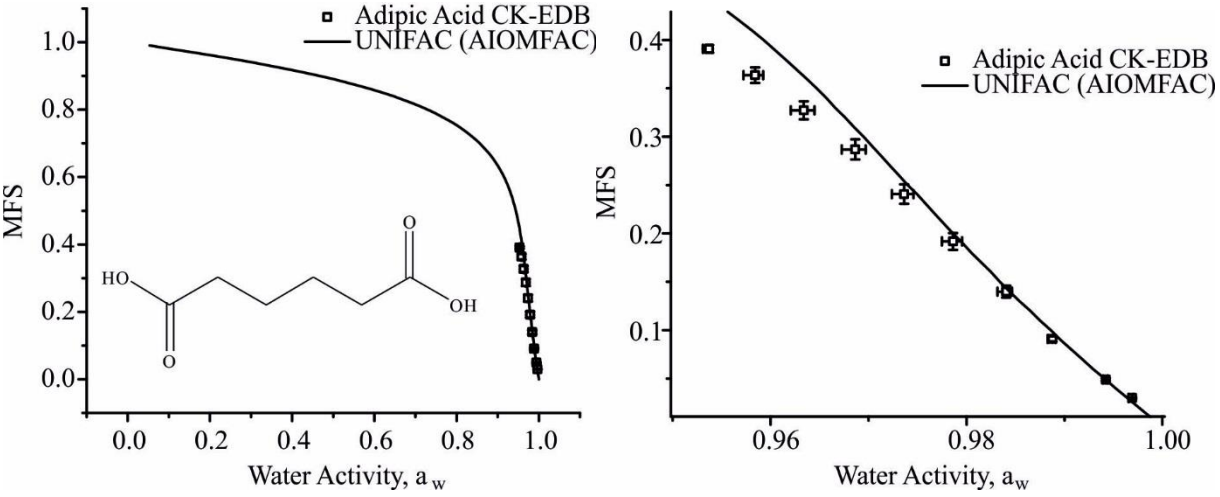

Table S15.1: Pure component refractive index (n_{melt}) is determined using molar refraction, assuming ideal mixing for calculation of the melt density (ρ_{melt}), from bulk data available in Cai et al. (2016). The variation of density as a function of the root of solute mass fraction ($MFS^{1/2} = x$) is represented by polynomial fit parameters. *Upper* and *lower* refer to 95 % confidence limits for fits to experimental data, (Section 2.2 in manuscript).

			Polynomial fit ($\rho_{sol} = a + b_1x + b_2x^2 + b_3x^3 + b_4x^4 + b_5x^5 + b_6x^6$)						
	n_{melt}	ρ_{melt}/ g.cm^{-3}	a	b_1	b_2	b_3	b_4	b_5	b_6
Best	1.5052	1.2897	998.2	-0.483	232.81	-36.78	137.06	-96.59	55.48
Upper	1.5093	1.3192	998.2	-0.705	253.36	-53.41	183.61	-139.01	77.14
Lower	1.5012	1.2614	998.2	-0.323	213.1	-24.73	101.55	-65.53	39.14

Table S15.2: Tabulated experimental data points shown in **Fig S15.1.**

a_w	error a_w (+ve)	error a_w (-ve)	MFS	error MFS
0.95373	3.22E-04	6.26E-04	0.39071	0.00391
0.95843	8.35E-04	0.00118	0.36348	0.00812
0.9634	0.0011	0.00133	0.3272	0.00935
0.96865	0.00107	0.00138	0.28685	0.01043
0.97365	9.42E-04	0.00127	0.24062	0.01007
0.97863	9.10E-04	0.00114	0.1917	0.00876
0.98405	5.88E-04	8.82E-04	0.13977	0.00621
0.98877	3.13E-04	4.91E-04	0.09086	0.0027
0.99423	1.80E-04	3.02E-04	0.04898	0.00153
0.99692	1.66E-04	3.62E-04	0.02978	7.74E-04

S16 Pimelic Acid Hygroscopicity

Fig S16.1: Hygroscopicity of Pimelic Acid, (Sigma Aldrich, Purity 99 %), at 293.15 K. Open squares, these experiments; solid line, UNIFAC model.

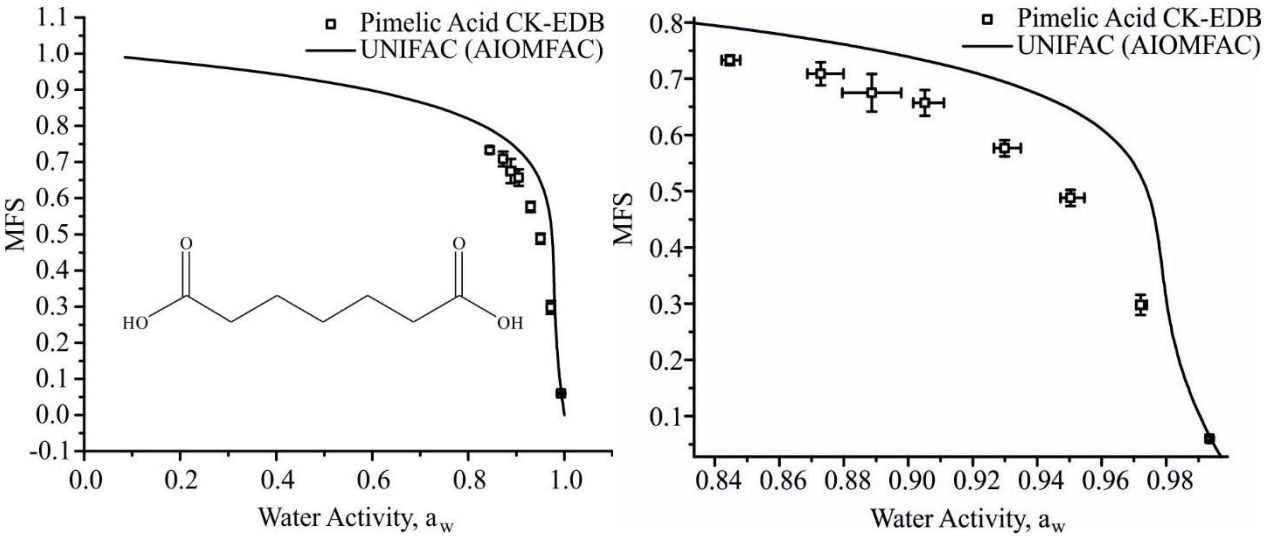

Table S16.1: Pure component refractive index (n_{melt}) is determined using molar refraction, assuming ideal mixing for calculation of the melt density (ρ_{melt}), from bulk data available in Cai et al. (2016). The variation of density as a function of the root of solute mass fraction ($MFS^{1/2} = x$) is represented by polynomial fit parameters. *Upper* and *lower* refer to 95 % confidence limits for fits to experimental data, (Section 2.2 in manuscript).

			Polynomial fit ($\rho_{sol} = a + b_1x + b_2x^2 + b_3x^3 + b_4x^4 + b_5x^5 + b_6x^6$)						
	n_{melt}	ρ_{melt}/ g.cm^{-3}	a	b_1	b_2	b_3	b_4	b_5	b_6
Best	1.4917	1.2262	998.5	-0.184	188.18	-14.19	67.86	-37.91	23.94
Upper	1.4940	1.2435	998.5	-0.246	200.41	-18.89	83.16	-50.18	30.74
Lower	1.4894	1.2095	998.5	-0.136	176.23	-10.52	55.25	-28.29	18.47

Table S16.2: Tabulated experimental data points shown in **Fig S16.1.**

a_w	error a_w (+ve)	error a_w (-ve)	MFS	error MFS
0.84466	0.00317	0.00251	0.73296	0.0087
0.87279	0.00711	0.00413	0.70863	0.02048
0.88863	0.00919	0.00916	0.67508	0.03342
0.90517	0.00585	0.00361	0.65697	0.02274
0.92985	0.00504	0.00334	0.57632	0.01441
0.9503	0.00434	0.00304	0.48806	0.01436
0.97207	0.0019	0.00139	0.29782	0.01787
0.99347	2.49E-04	3.32E-04	0.06002	0.00268

S17 Methyl Malonic Acid Hygroscopicity

Fig S17.1: Hygroscopicity of methyl malonic acid, (Sigma Aldrich, Purity 99 %), at 293.15 K. Open squares, these experiments; solid line, UNIFAC model.

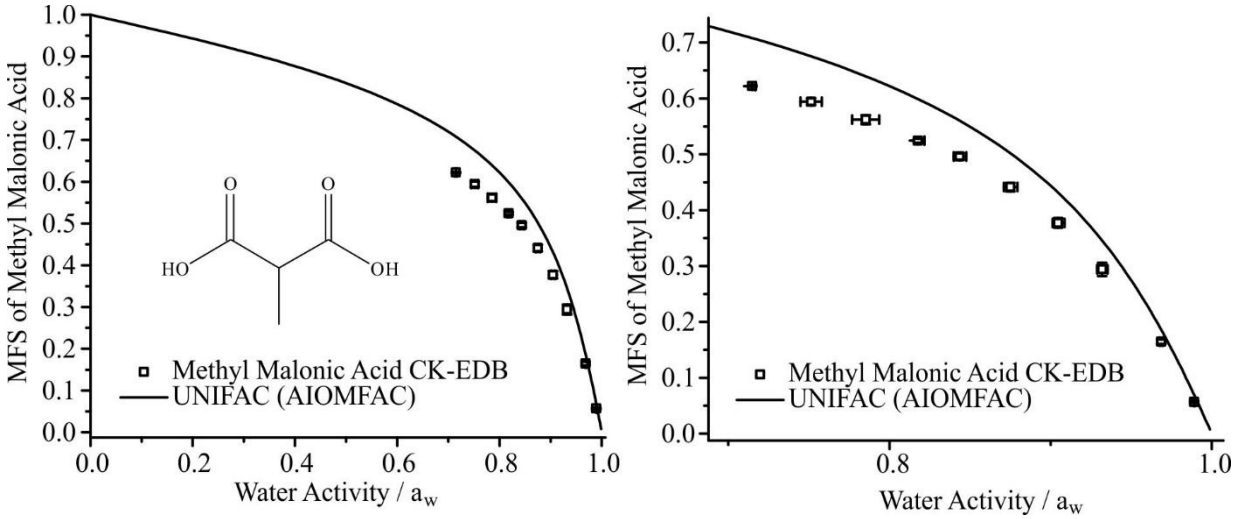

Table S17.1: Pure component refractive index (n_{melt}) is determined using molar refraction, assuming ideal mixing for calculation of the melt density (ρ_{melt}), from bulk data available in Cai et al. (2016). The variation of density as a function of the root of solute mass fraction ($MFS^{1/2}$ =x) is represented by polynomial fit parameters. *Upper* and *lower* refer to 95 % confidence limits for fits to experimental data, (Section 2.2 in manuscript).

			Polynomial fit ($\rho_{sol} = a + b_1x + b_2x^2 + b_3x^3 + b_4x^4 + b_5x^5 + b_6x^6$)						
	n_{melt}	ρ_{melt}/ $g.cm^{-3}$	a	b_1	b_2	b_3	b_4	b_5	b_6
Best	1.4817	1.3876	998.8	-1.45	301.28	-108.73	330.65	-279.56	146.61
Upper	1.4819	1.3902	998.8	-1.49	303.18	-111.53	337.82	-286.56	149.98
Lower	1.4815	1.3851	998.8	-1.42	299.45	-106.09	323.86	-272.94	143.43

Table S17.2: Tabulated experimental data points shown in **Fig S17.1.**

a_w	error a_w (+ve)	error a_w (-ve)	MFS	error MFS
0.71493	0.002	0.00248	0.62219	0.00155
0.75141	0.00657	0.00657	0.59428	0.00609
0.78527	0.0084	0.0084	0.562	0.00836
0.81777	0.004	0.00245	0.52434	0.00364
0.84355	0.00409	0.00369	0.49609	0.00573
0.875	0.00438	0.00401	0.44143	0.00784
0.90462	0.00402	0.00333	0.3774	0.00875
0.93201	0.00335	0.00317	0.29413	0.01184
0.96865	8.29E-04	8.90E-04	0.16472	0.0041
0.98911	4.09E-04	4.11E-04	0.05691	0.00203

S18 Methyl Succinic Acid Hygroscopicity

Figure S18.1: Hygroscopicity of methyl succinic acid, (Sigma Aldrich, Purity 99 %), at 293.15 K. Open squares, these experiments; solid line, UNIFAC model.

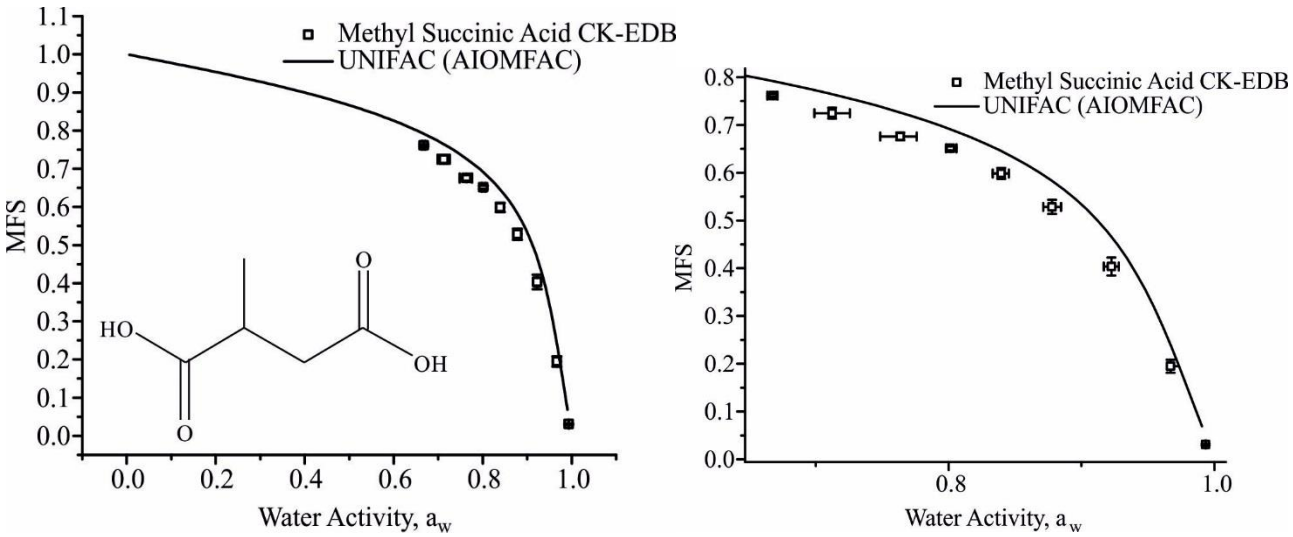

Table S18.1: Pure component refractive index (n_{melt}) is determined using molar refraction, assuming ideal mixing for calculation of the melt density (ρ_{melt}), from bulk data available in Cai et al. (2016). The variation of density as a function of the root of solute mass fraction ($MFS^{1/2} = x$) is represented by polynomial fit parameters. *Upper* and *lower* refer to 95 % confidence limits for fits to experimental data, (Section 2.2 in manuscript).

			Polynomial fit ($\rho_{sol} = a + b_1x + b_2x^2 + b_3x^3 + b_4x^4 + b_5x^5 + b_6x^6$)						
	n_{melt}	ρ_{melt}/ $g.cm^{-3}$	a	b_1	b_2	b_3	b_4	b_5	b_6
Best	1.4779	1.3035	998.2	-0.572	242.3	-43.51	156.55	-114.16	64.69
Upper	1.4784	1.3090	998.2	-0.614	246.13	-46.62	165.26	-122.12	68.76
Lower	1.4774	1.2980	998.2	-0.533	238.48	-40.56	148.19	-106.58	60.79

Table S18.2: Tabulated experimental data points shown in **Fig S18.1.**

a_w	error a_w (+ve)	error a_w (-ve)	MFS	error MFS
0.66772	0.00345	0.00424	0.76125	0.00296
0.71234	0.0134	0.0134	0.72476	0.01132
0.7636	0.01237	0.01517	0.67596	0.00785
0.80135	0.00451	0.00326	0.65118	0.00447
0.83951	0.00575	0.00629	0.59855	0.01151
0.87778	0.00688	0.00657	0.52839	0.01469
0.92249	0.00567	0.00567	0.40343	0.01891
0.96705	0.00282	0.00249	0.19484	0.01368
0.99344	3.28E-04	3.47E-04	0.03075	0.00168

S19 Binary Aqueous Diethylmalonic Acid - Hygroscopicity

Fig S19.1: Hygroscopicity of diethylmalonic acid, (Sigma Aldrich, Purity 98 %), at 293.15 K. Open squares, these experiments; solid line, UNIFAC model.

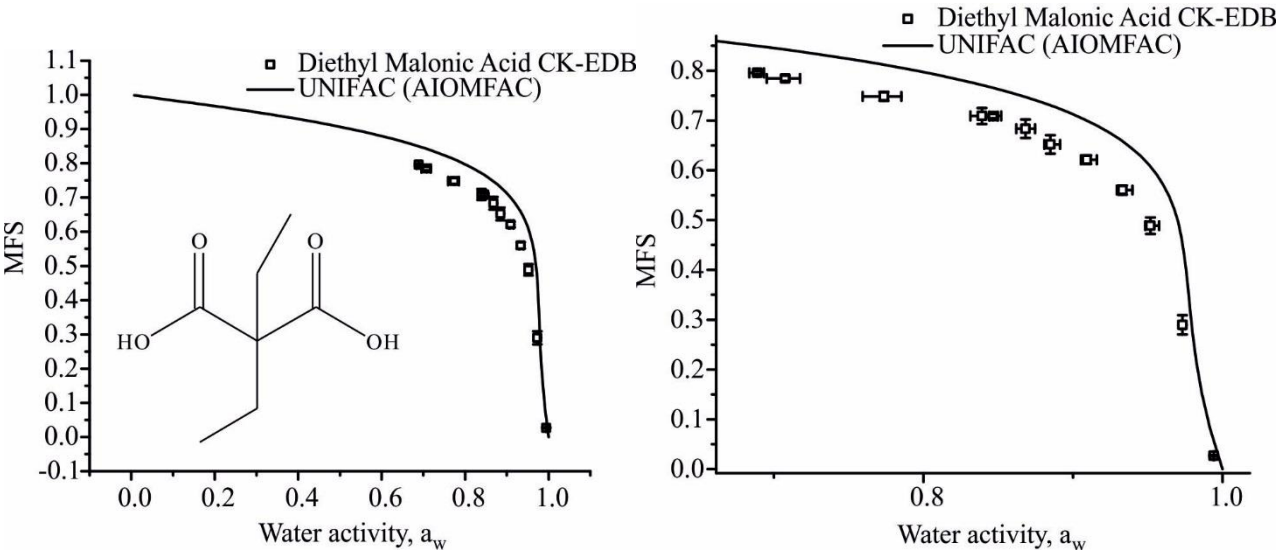

Table S19.1: Pure component refractive index (n_{melt}) is determined using molar refraction, assuming ideal mixing for calculation of the melt density (ρ_{melt}), from bulk data available in Cai et al. (2016). The variation of density as a function of the root of solute mass fraction ($MFS^{1/2} = x$) is represented by polynomial fit parameters. *Upper* and *lower* refer to 95 % confidence limits for fits to experimental data, (Section 2.2 in manuscript).

			Polynomial fit ($\rho_{sol} = a + b_1x + b_2x^2 + b_3x^3 + b_4x^4 + b_5x^5 + b_6x^6$)						
	n_{melt}	ρ_{melt}/ $g.cm^{-3}$	a	b_1	b_2	b_3	b_4	b_5	b_6
Best	1.4854	1.2184	998.2	-0.161	182.82	-12.45	61.98	-33.36	21.37
Upper	1.4858	1.2219	998.2	-0.172	185.32	-13.25	64.69	-35.44	22.55
Lower	1.4850	1.2149	998.2	-0.151	180.32	-11.69	59.36	-31.37	20.24

Table S19.2: Tabulated experimental data points shown in **Figure S19.1.**

a_w	error a_w (+ve)	error a_w (-ve)	MFS	error MFS
0.68895	0.00441	0.00543	0.79565	0.00315
0.70762	0.01	0.01233	0.78448	0.00548
0.7737	0.01156	0.01425	0.7484	0.00901
0.83916	0.01287	0.00773	0.70902	0.01617
0.84654	0.00329	0.00246	0.70885	0.00435
0.86832	0.00637	0.0062	0.68324	0.01847
0.88499	0.00646	0.00418	0.65203	0.0186
0.90928	0.00665	0.00391	0.62123	0.00847
0.93317	0.00665	0.00374	0.56028	0.00907
0.95177	0.00586	0.00329	0.48861	0.01646
0.97321	0.00199	0.00152	0.28968	0.01912
0.99422	3.23E-04	3.66E-04	0.02697	0.00157

S20 2,2-Dimethyl Glutaric Acid Hygroscopicity

Fig S20.1: Hygroscopicity of 2,2-dimethyl glutaric acid, (Sigma Aldrich, Purity > 98 %), at 293.15 K. Open squares, these experiments; solid line, UNIFAC model.

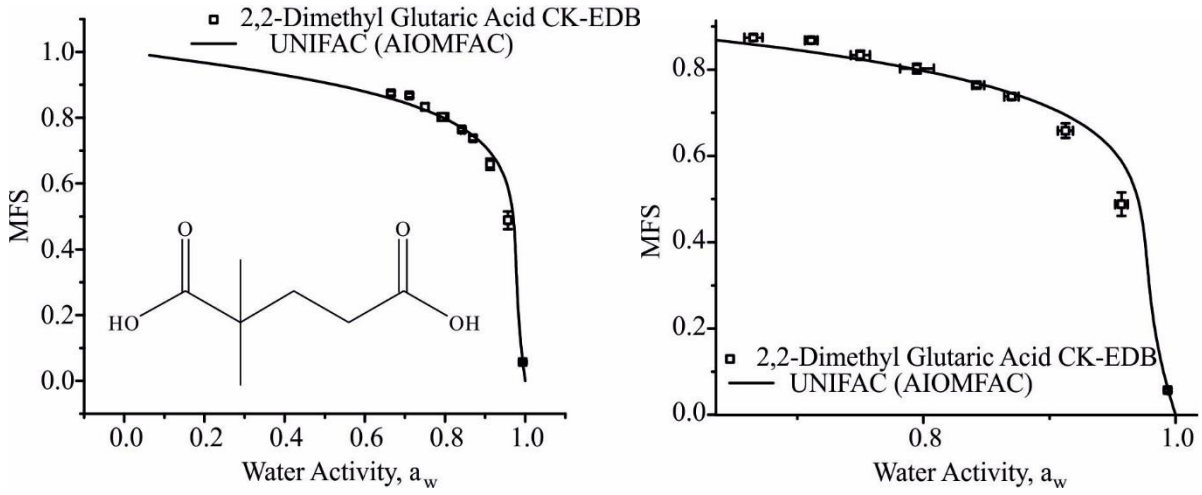

Table S20.1: Pure component refractive index (n_{melt}) is determined using molar refraction, assuming ideal mixing for calculation of the melt density (ρ_{melt}), from bulk data available in Cai et al. (2016). The variation of density as a function of the root of solute mass fraction ($MFS^{1/2}$ =x) is represented by polynomial fit parameters. *Upper* and *lower* refer to 95 % confidence limits for fits to experimental data, (Section 2.2 in manuscript).

			Polynomial fit ($\rho_{sol} = a + b_1x + b_2x^2 + b_3x^3 + b_4x^4 + b_5x^5 + b_6x^6$)						
	n_{melt}	ρ_{melt}/ $g.cm^{-3}$	a	b_1	b_2	b_3	b_4	b_5	b_6
Best	1.4881	1.2225	998.2	-0.174	185.75	-13.39	65.16	-35.81	22.76
Upper	1.4884	1.2248	998.2	-0.181	187.39	-13.93	67	-37.24	23.57
Lower	1.4878	1.2201	998.2	-0.166	184.04	-12.83	63.28	-34.36	21.94

Table S19.2: Tabulated experimental data points shown in **Fig S20.1.**

a_w	error a_w (+ve)	error a_w (-ve)	MFS	error MFS
0.66522	0.00707	0.00713	0.87406	0.00722
0.71105	0.00493	0.00494	0.8677	0.00654
0.74996	0.00758	0.00758	0.83334	0.01058
0.79488	0.01337	0.01338	0.80256	0.01126
0.84249	0.00573	0.00389	0.76365	0.00522
0.86987	0.00563	0.00574	0.73768	0.00728
0.91262	0.00592	0.00605	0.65854	0.01692
0.95695	0.00508	0.00491	0.48805	0.02723
0.99362	3.59E-04	3.74E-04	0.05685	0.00348

S21 2,2-Dimethyl Succinic Acid Hygroscopicity

Fig S21.1: Hygroscopicity of 2,2-dimethyl succinic acid, (Sigma Aldrich, Purity 99 %), at 293.15 K. Open squares, these experiments; solid line, UNIFAC model.

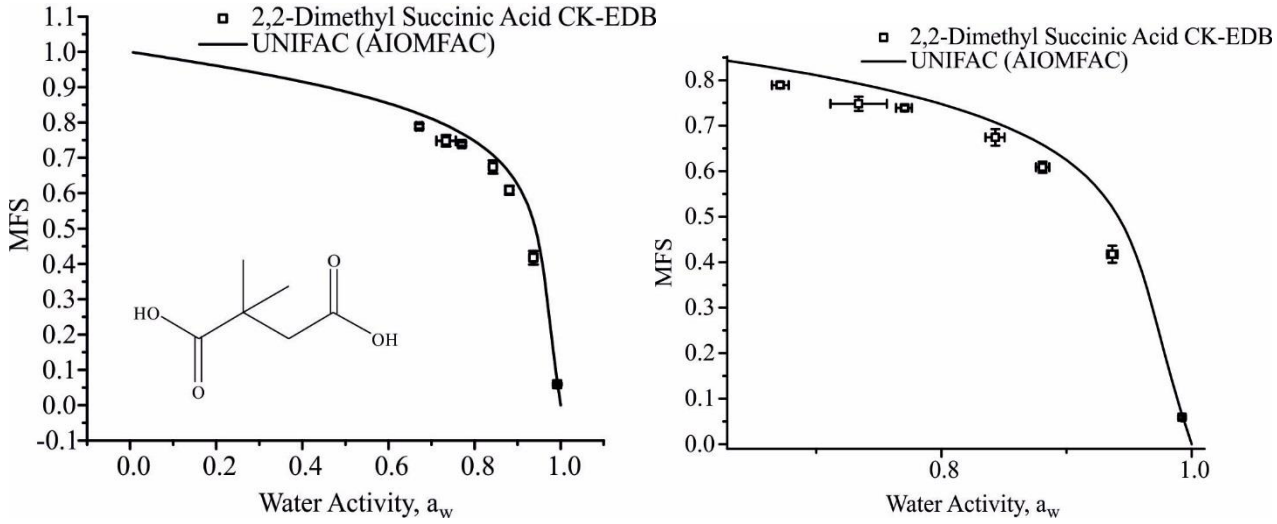

Table S21.1: Pure component refractive index (n_{melt}) is determined using molar refraction, assuming ideal mixing for calculation of the melt density (ρ_{melt}), from bulk data available in Cai et al. (2016). The variation of density as a function of the root of solute mass fraction ($MFS^{1/2}$ =x) is represented by polynomial fit parameters. *Upper* and *lower* refer to 95 % confidence limits for fits to experimental data, (Section 2.2 in manuscript).

			Polynomial fit ($\rho_{sol} = a + b_1x + b_2x^2 + b_3x^3 + b_4x^4 + b_5x^5 + b_6x^6$)						
	n_{melt}	ρ_{melt}/ $g.cm^{-3}$	a	b_1	b_2	b_3	b_4	b_5	b_6
Best	1.4889	1.2710	997.9	-0.382	220.13	-29.13	114.09	-76.29	44.68
Upper	1.4897	1.2776	997.9	-0.419	224.73	-31.96	122.4	-83.53	48.48
Lower	1.4880	1.2644	997.9	-0.347	215.51	-26.48	106.23	-69.5	41.09

Table S21.2: Tabulated experimental data points shown in **Fig S21.1**

a_w	error a_w (+ve)	error a_w (-ve)	MFS	error MFS
0.6713	0.00663	0.00663	0.78921	0.00655
0.73389	0.02256	0.02256	0.74829	0.01579
0.77076	0.00564	0.00705	0.73908	0.00579
0.84308	0.00747	0.00776	0.67413	0.01818
0.88089	0.00536	0.00529	0.60846	0.01212
0.9367	0.00425	0.00424	0.41751	0.01893
0.99244	4.24E-04	5.93E-04	0.05911	0.00313

S22 2-Methyl Glutaric Acid Hygroscopicity

Fig S22.1: Hygroscopicity of 2-methyl glutaric acid, (Sigma Aldrich, Purity 98 %), at 293.15 K. Open squares, these experiments; solid line, UNIFAC model.

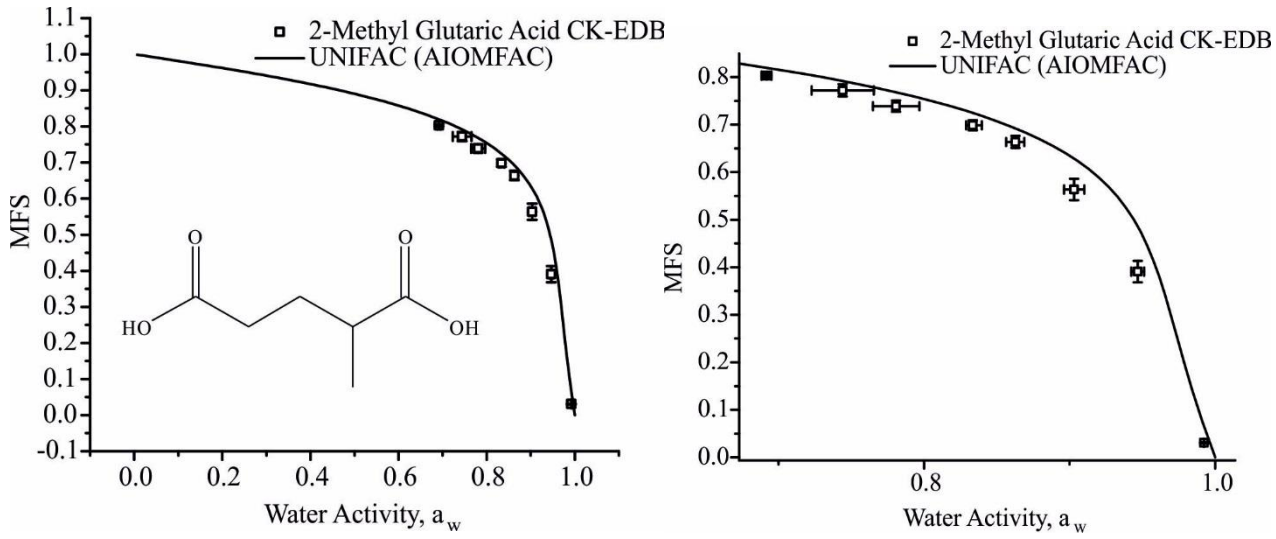

Table S22.1: Pure component refractive index (n_{melt}) is determined using molar refraction, assuming ideal mixing for calculation of the melt density (ρ_{melt}), from bulk data available in Cai et al. (2016). The variation of density as a function of the root of solute mass fraction ($MFS^{1/2}$ =x) is represented by polynomial fit parameters. *Upper* and *lower* refer to 95 % confidence limits for fits to experimental data, (Section 2.2 in manuscript).

			Polynomial fit ($\rho_{sol} = a + b_1x + b_2x^2 + b_3x^3 + b_4x^4 + b_5x^5 + b_6x^6$)						
	n_{melt}	ρ_{melt}/ $g.cm^{-3}$	a	b_1	b_2	b_3	b_4	b_5	b_6
Best	1.4866	1.2585	997.6	-0.319	211.59	-24.4	99.95	-64.16	38.24
Upper	1.4873	1.2648	997.6	-0.350	216	-26.78	107.1	-70.26	41.49
Lower	1.4858	1.2522	997.6	-0.290	207.17	-22.18	93.17	-58.44	35.17

Table S22.2: Tabulated experimental data points shown in **Fig S22.1**

a_w	error a_w (+ve)	error a_w (-ve)	MFS	error MFS
0.68925	0.00271	0.00334	0.80479	0.00208
0.72204	0.01005	0.01239	0.78383	0.00857
0.76123	0.01296	0.01422	0.75567	0.01704
0.78959	0.02339	0.02377	0.73478	0.02713
0.82836	0.01185	0.00726	0.70077	0.02018
0.84699	0.00634	0.00601	0.68658	0.01104
0.8785	0.00611	0.00622	0.63205	0.01527
0.91076	0.00612	0.00583	0.54437	0.02194
0.94004	0.00438	0.00438	0.4312	0.02071
0.98128	4.79E-04	0.0012	0.14884	0.0113
0.99285	2.24E-04	2.25E-04	0.02928	0.00106

S23 3-Methyl Adipic Acid Hygroscopicity

Fig S23.1: Hygroscopicity of 3-methyl adipic acid, (Sigma Aldrich, Purity 99 %), at 293.15 K. Open squares, these experiments; solid line, UNIFAC model.

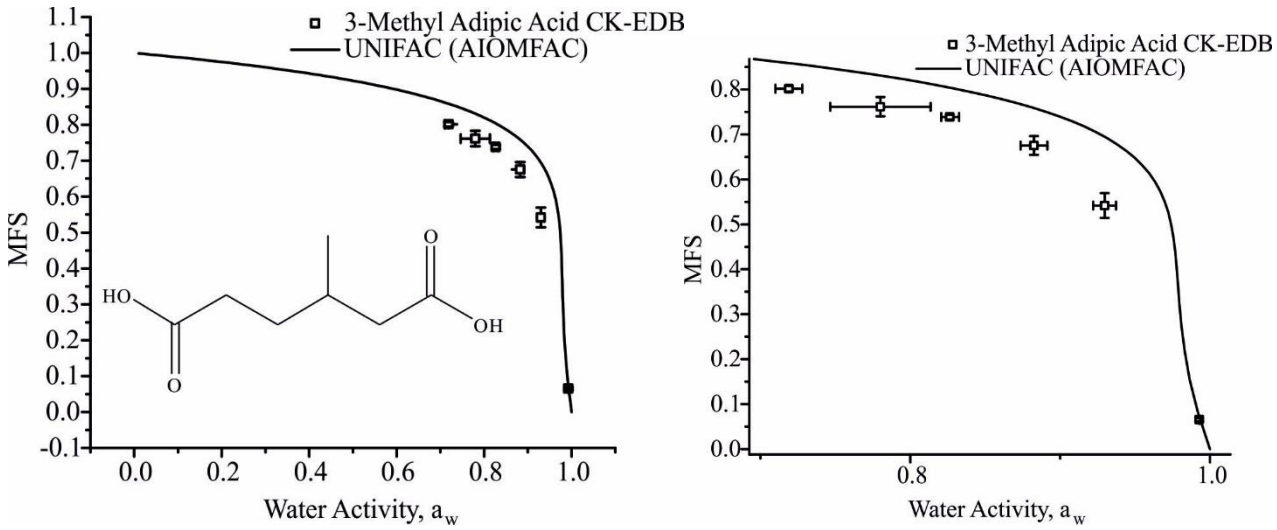

Table S23.1: Pure component refractive index (n_{melt}) is determined using molar refraction, assuming ideal mixing for calculation of the melt density (ρ_{melt}), from bulk data available in Cai et al. (2016). The variation of density as a function of the root of solute mass fraction ($MFS^{1/2} = x$) is represented by polynomial fit parameters. *Upper* and *lower* refer to 95 % confidence limits for fits to experimental data, (Section 2.2 in manuscript).

			Polynomial fit ($\rho_{sol} = a + b_1x + b_2x^2 + b_3x^3 + b_4x^4 + b_5x^5 + b_6x^6$)						
	n_{melt}	ρ_{melt}/ $g.cm^{-3}$	a	b_1	b_2	b_3	b_4	b_5	b_6
Best	1.4865	1.2141	999.0	-0.147	179.19	-11.33	58.11	-30.42	19.69
Upper	1.4878	1.2243	999.0	-0.176	186.48	-13.59	65.86	-36.34	23.06
Lower	1.4852	1.2041	999.0	-0.121	171.99	-9.4	51.21	-25.33	16.75

Table S23.2: Tabulated experimental data points shown in **Fig S23.1.**

a_w	error a_w (+ve)	error a_w (-ve)	MFS	error MFS
0.71902	0.00897	0.00897	0.80154	0.00624
0.78015	0.03348	0.03347	0.7615	0.02149
0.82646	0.00615	0.00574	0.73848	0.00556
0.88266	0.00886	0.00907	0.67532	0.02097
0.92986	0.00748	0.00771	0.54185	0.02748
0.993	2.61E-04	3.72E-04	0.06527	0.00354

S24 3-Methyl Glutaric Acid Hygroscopicity

Fig S24.1: Hygroscopicity of 3-methyl glutaric acid, (Sigma Aldrich, Purity 99 %), at 293.15 K. Open squares, these experiments; solid line, UNIFAC model.

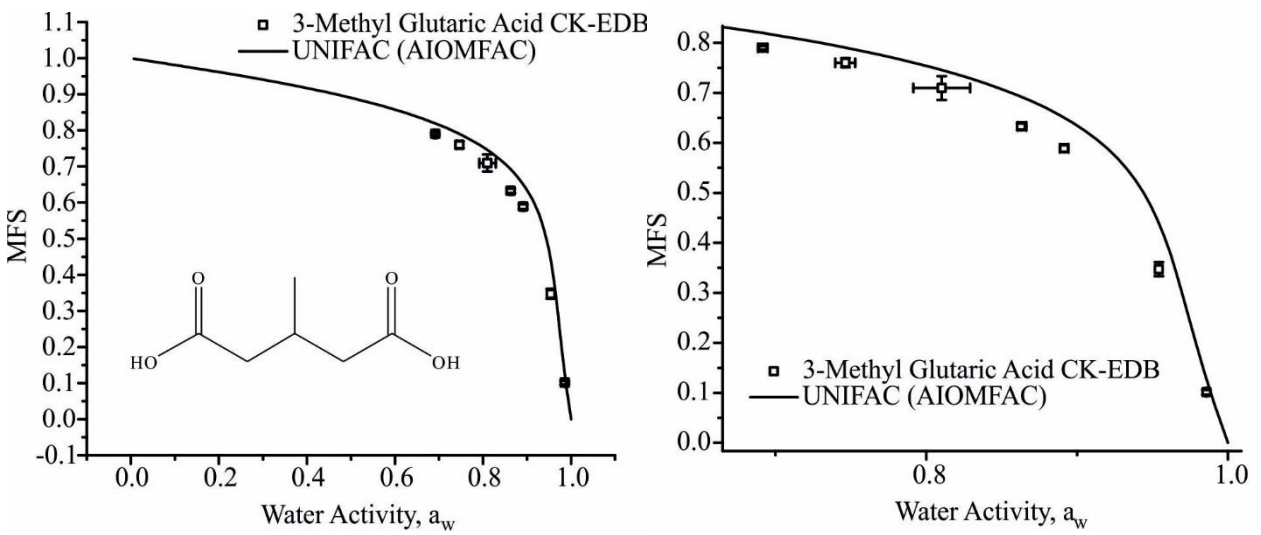

Table SI.24.1: Pure component refractive index (n_{melt}) is determined using molar refraction, assuming ideal mixing for calculation of the melt density (ρ_{melt}), from bulk data available in Cai et al. (2016). The variation of density as a function of the root of solute mass fraction ($MFS^{1/2} = x$) is represented by polynomial fit parameters. *Upper* and *lower* refer to 95 % confidence limits for fits to experimental data, (Section 2.2 in manuscript).

			Polynomial fit ($\rho_{sol} = a + b_1x + b_2x^2 + b_3x^3 + b_4x^4 + b_5x^5 + b_6x^6$)						
	n_{melt}	ρ_{melt}/ $g.cm^{-3}$	a	b_1	b_2	b_3	b_4	b_5	b_6
Best	1.4819	1.2498	997.9	-0.277	205.29	-21.26	90.32	-56.07	33.89
Upper	1.4822	1.2531	997.9	-0.292	207.6	-22.37	93.74	-58.92	35.43
Lower	1.4816	1.2466	997.9	-0.264	203.04	-20.22	87.1	-53.39	32.44

Table S24.2: Tabulated experimental data points shown in **Fig S24.1.**

a_w	error a_w (+ve)	error a_w (-ve)	MFS	error MFS
0.69173	0.00299	0.00334	0.79013	0.0038
0.74649	0.00642	0.00683	0.76025	0.00932
0.81013	0.01887	0.01884	0.70959	0.02367
0.86283	0.00343	0.00213	0.63276	0.00618
0.89131	0.00283	0.00283	0.58884	0.00675
0.95411	0.00246	0.00245	0.3472	0.01394
0.98567	6.06E-04	6.09E-04	0.10123	0.00477

S25 3, 3-Dimethyl Glutaric Acid Hygroscopicity

Fig S25.1: Hygroscopicity of 3, 3-dimethyl glutaric acid, (Sigma Aldrich, Purity 98 %), at 293.15 K. Open squares, these experiments; solid line, UNIFAC model.

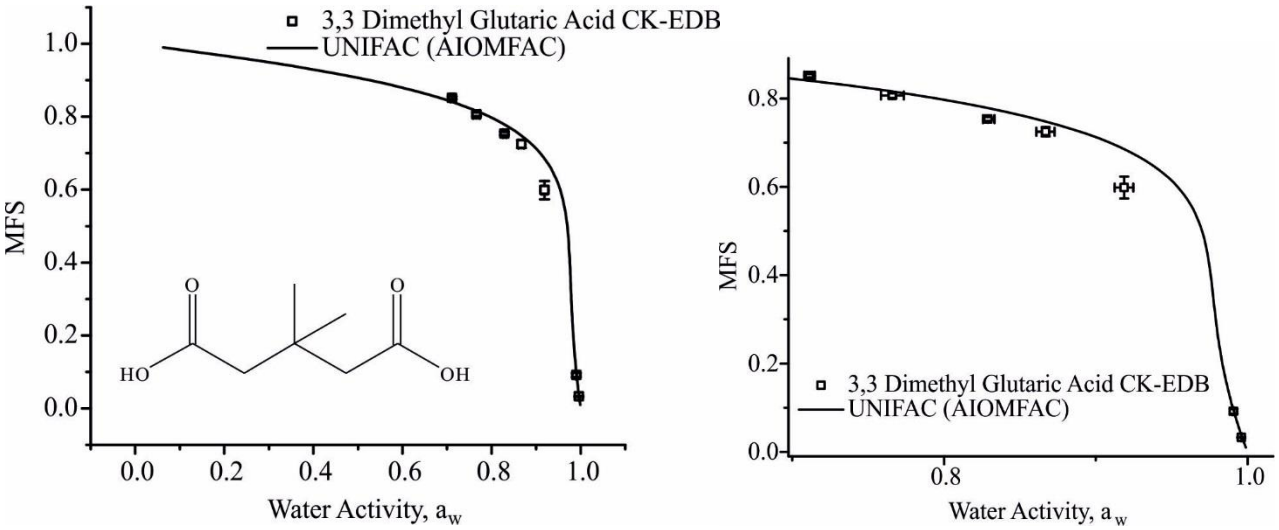

Table S25.1: Pure component refractive index (n_{melt}) is determined using molar refraction, assuming ideal mixing for calculation of the melt density (ρ_{melt}), from bulk data available in Cai et al. (2016). The variation of density as a function of the root of solute mass fraction ($MFS^{1/2} = x$) is represented by polynomial fit parameters. *Upper* and *lower* refer to 95 % confidence limits for fits to experimental data, (Section 2.2 in manuscript).

			Polynomial fit ($\rho_{sol} = a + b_1x + b_2x^2 + b_3x^3 + b_4x^4 + b_5x^5 + b_6x^6$)						
	n_{melt}	ρ_{melt}/ $g.cm^{-3}$	a	b_1	b_2	b_3	b_4	b_5	b_6
Best	1.4903	1.2206	998.3	-0.167	184.33	-12.92	63.58	-34.59	22.07
Upper	1.4906	1.2231	998.3	-0.175	186.11	-13.5	65.55	-36.11	22.93
Lower	1.4900	1.2182	998.3	-0.160	182.61	-12.38	61.74	-33.18	21.27

Table S25.2: Tabulated experimental data points shown in **Fig S25.1.**

a_w	error a_w (+ve)	error a_w (-ve)	MFS	error MFS
0.71132	0.00345	0.00345	0.85176	0.00384
0.76078	0.006	0.00743	0.80912	0.00721
0.79151	0.01941	0.01942	0.79788	0.01562
0.83444	0.00416	0.00451	0.75169	0.00421
0.87055	0.00543	0.00565	0.71882	0.0105
0.91582	0.00545	0.00564	0.61641	0.02163
0.96018	0.00389	0.00389	0.39161	0.02576
0.99443	2.18E-04	2.83E-04	0.04485	0.00225

S26. PEG3 Hygroscopicity

Fig S26.1: Hygroscopicity of PEG3, at 293.15 K. Open squares, these experiments; solid line, UNIFAC model.

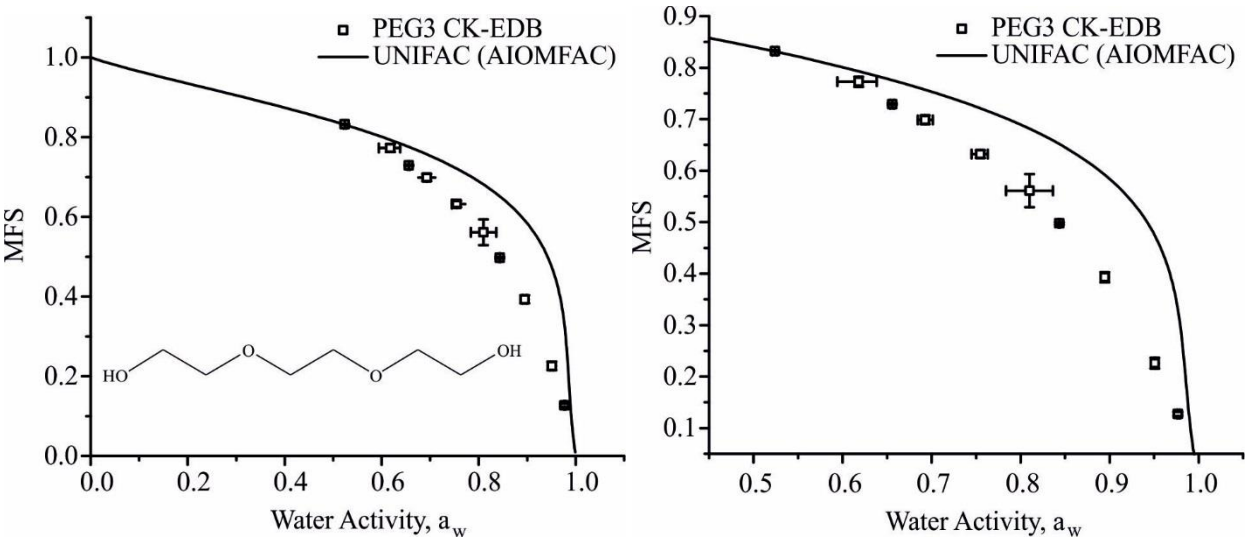

Table S26.1: Measured values of pure component melt density (ρ_{melt}) and refractive index (n_{melt}) (PEG3 is liquid), presented with parameterisation for solution measurements of density where x is the square root of MFS ($MFS^{1/2}$ =x). *Upper* and *lower* refer to 95 % confidence limits for fits to experimental data. Upper and lower limit on refractive index and density are determined by the error in the refractometer and by the densitometer respectively.

			Polynomial fit ($\rho_{sol} = a + b_1x + b_2x^2 + b_3x^3$)			
	n_{melt}	ρ_{melt}/ g.cm^{-3}	a	b_1	b_2	b_3
Best	1.4551	1.109	999.97	-75.75	431.63	-246.73
Upper	1.4552	1.122	999.97	-0.198	268.11	-144.15
Lower	1.4550	1.096	999.97	-151.31	595.15	-349.31

Table S26.2: Tabulated experimental data points shown in **Fig S26.1.**

a_w	error a_w (+ve)	error a_w (-ve)	MFS	error MFS
0.524	0.0024	0.00286	0.83232	0.00127
0.61806	0.02008	0.02389	0.77269	0.0098
0.65597	0.00198	0.00242	0.72923	0.00152
0.69291	0.00856	0.00856	0.69867	0.0088
0.75489	8.16E-03	0.01	0.63211	7.82E-03
0.81001	0.0263	0.0263	0.56113	0.03211
0.84347	0.00123	0.00119	0.49753	0.00229
0.89472	0.00416	0.00414	0.39303	0.01004
0.95087	3.07E-03	3.07E-03	0.22603	0.01048
0.97688	0.00201	0.00112	0.12742	0.00393

S27. PEG4 Hygroscopicity

Fig S27.1: Hygroscopicity of PEG4, at 293.15 K. Open squares, these CC-EDB experiments; solid line, UNIFAC model; blue line UManSysProp; red line adsorption isotherm model from Dutcher.

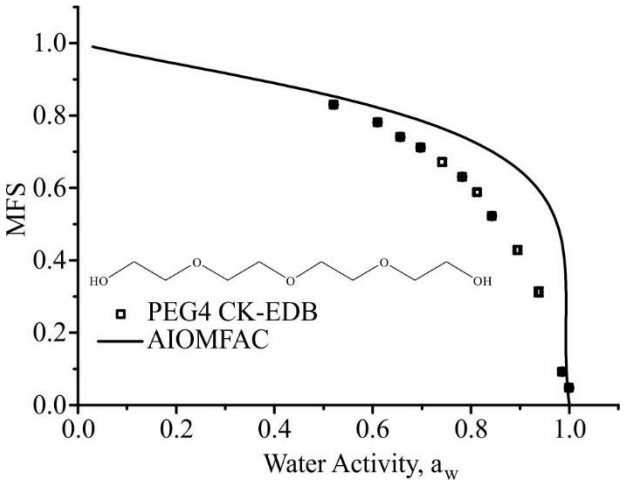

Table S27.1: Measured values of pure component melt density (ρ_{melt}) and refractive index (n_{melt}) (PEG4 is liquid), presented with parameterisation for solution measurements of density where x is the square root of MFS ($MFS^{1/2}$ =x). *Upper* and *lower* refer to 95 % confidence limits for fits to experimental data. Upper and lower limit on refractive index and density are determined by the error in the refractometer and by the densitometer respectively.

			Polynomial fit ($\rho_{sol} = a + b_1x + b_2x^2 + b_3x^3$)			
	n_{melt}	ρ_{melt}/ g.cm^{-3}	a	b_1	b_2	b_3
Best	1.4589	1.1271	999.97	-37.39	296.85	-130.68
Upper	1.4590	1.13412	999.97	-9.65	235.84	-92.25
Lower	1.4588	1.12338	999.97	-65.13	357.86	-169.11

Table S27.2: Tabulated experimental data points shown in **Fig S27.1.**

a_w	error a_w (+ve)	error a_w (-ve)	MFS	error MFS
0.52052	0.00336	0.00399	0.83006	8.065E-4
0.60966	0.00229	0.00278	0.78149	8.220E-4
0.65636	0.00166	0.00204	0.74058	0.00177
0.69735	0.00172	0.00212	0.71195	0.00154
0.74132	0.00556	0.00685	0.67145	0.00929
0.78212	6.975E-4	8.803E-4	0.63073	8.501E-4
0.81258	0.00536	0.00535	0.58791	0.00759
0.84243	0.00132	0.00111	0.52225	0.00213
0.89453	0.00427	0.00448	0.42827	0.01048
0.93766	0.00385	0.00376	0.31263	0.01217
0.98571	0.0013	0.00127	0.0918	0.00662
0.99969	0.00143	0.00156	0.0475	0.00252

S28 Erythritol Hygroscopicity

Fig S28.1: Hygroscopicity of erythritol (Sigma Aldrich 99 %), at 293.15 K. Open squares, these experiments; solid line, UNIFAC model.

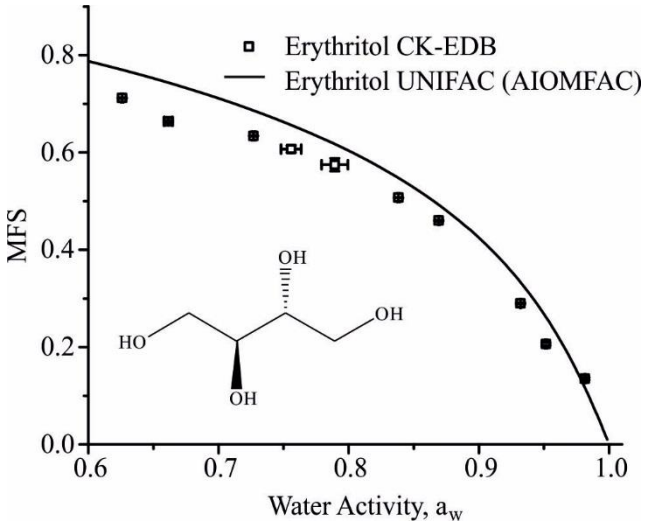

Table S28.1: Pure component refractive index (n_{melt}) is determined using molar refraction, assuming ideal mixing for calculation of the melt density (ρ_{melt}), from bulk data available in Cai et al. (2016). The variation of density as a function of the root of solute mass fraction ($MFS^{1/2} = x$) is represented by polynomial fit parameters. *Upper* and *lower* refer to 95 % confidence limits for fits to experimental data, (Section 2.2 in manuscript).

			Polynomial fit ($\rho_{sol} = a + b_1x + b_2x^2 + b_3x^3$)			
	n_{melt}	ρ_{melt}/ g.cm^{-3}	a	b_1	b_2	b_3
Best	1.5211	1.3754	998.6	58.46	37.98	278.66
Upper	1.5388	1.3813	998.6	60.21	33.79	286.94
Lower	1.5204	1.3695	998.6	56.75	42.03	27.049

Table S28.2: Tabulated experimental data points shown in **Fig S28.1.**

a_w	error a_w (+ve)	error a_w (-ve)	MFS	error MFS
0.62602	8.77112E-4	0.00107	0.71188	6.08334E-4
0.66147	0.0027	0.0033	0.66395	0.00226
0.72692	0.00104	0.00129	0.6342	6.57702E-4
0.75582	0.00775	0.00777	0.60723	0.00739
0.78929	0.01009	0.0101	0.57499	0.01315
0.83827	7.77253E-4	0.001	0.50705	9.72437E-4
0.86916	7.13427E-4	6.96511E-4	0.46004	0.00138
0.93195	2.64028E-4	3.52642E-4	0.28987	0.00175
0.95145	7.53773E-4	7.52526E-4	0.20621	0.00312
0.9815	5.76107E-4	5.56581E-4	0.13503	0.00279

S29 Sorbitol Hygroscopicity

Fig S29.1: Hygroscopicity of sorbitol (Sigma Aldrich ≥ 98 %), at 293.15 K. Open squares, these experiments; solid line, UNIFAC model. Data taken at RHs lower than indicated by the dashed black line show increased error in hygroscopicity retrieval due to the imposition of a kinetic limitation on water transport.

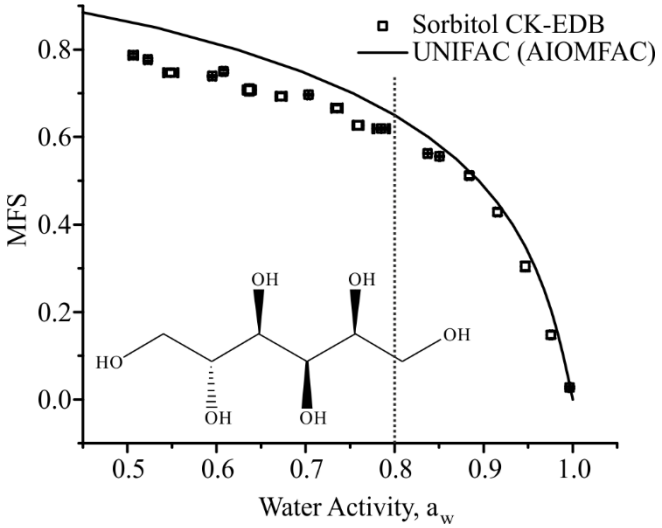

Table S29.1: Pure component refractive index (n_{melt}) determined using molar refraction where the melt density (ρ_{melt}) is determined using a polynomial fit of density to the square root of MFS ($MFS^{1/2}$ =x). Bulk values used are available in Cai et al. (2016). *Upper* and *lower* refer to 95 % confidence limits for fits to experimental data.

			Polynomial fit ($\rho_{sol} = a + b_1x + b_2x^2 + b_3x^3$)			
	n_{melt}	ρ_{melt}/ g.cm^{-3}	a	b_1	b_2	b_3
Best	1.5244	1.4231	997.8	8.6	286.1	130.7
Upper	1.5267	1.4333	997.8	24.74	234.56	175.54
Lower	1.5220	1.4128	997.8	-7.6	337.59	85.83

Table S29.2: Tabulated experimental data points shown in **Fig S29.1.**

a_w	error a_w (+ve)	error a_w (-ve)	MFS	error MFS
0.50647	0.00432	0.00512	0.78667	0.00341
0.52291	0.0031	0.00369	0.7771	0.00307
0.54873	0.00705	0.00838	0.74672	0.00731
0.59535	0.00322	0.00389	0.73916	0.00193
0.60809	0.0019	0.0023	0.74976	0.00343
0.63682	0.00605	0.00728	0.70773	0.01216
0.67255	0.00497	0.00601	0.69271	0.00773
0.7035	0.00148	0.00183	0.69648	0.00163
0.73531	0.00619	0.00619	0.66608	0.00694
0.75896	0.00493	0.00599	0.62673	0.00941
0.78492	0.00775	0.00958	0.61901	0.00237
0.83722	0.00384	0.0025	0.56241	9.55991E-4
0.85049	9.622E-4	8.165E-4	0.5556	0.00118
0.88386	0.00262	0.0027	0.51154	0.00629
0.91574	0.00253	0.00266	0.4286	0.0076
0.94681	0.00245	0.00245	0.30429	0.01053
0.97555	0.0014	0.00139	0.14769	0.00774
0.99655	0.00112	6.78573E-4	0.02751	0.00293

S30 D-(+)-Trehalose Dihydrate Hygroscopicity

Fig S30.1: Hygroscopicity of D-(+)-trehalose dihydrate (Sigma Aldrich ≥ 99 %), at 293.15 K. Open squares, these experiments; solid line, UNIFAC model. Data taken at RHs lower than indicated by the dashed black line show increased error in hygroscopicity retrieval due to the imposition of a kinetic limitation on water transport.

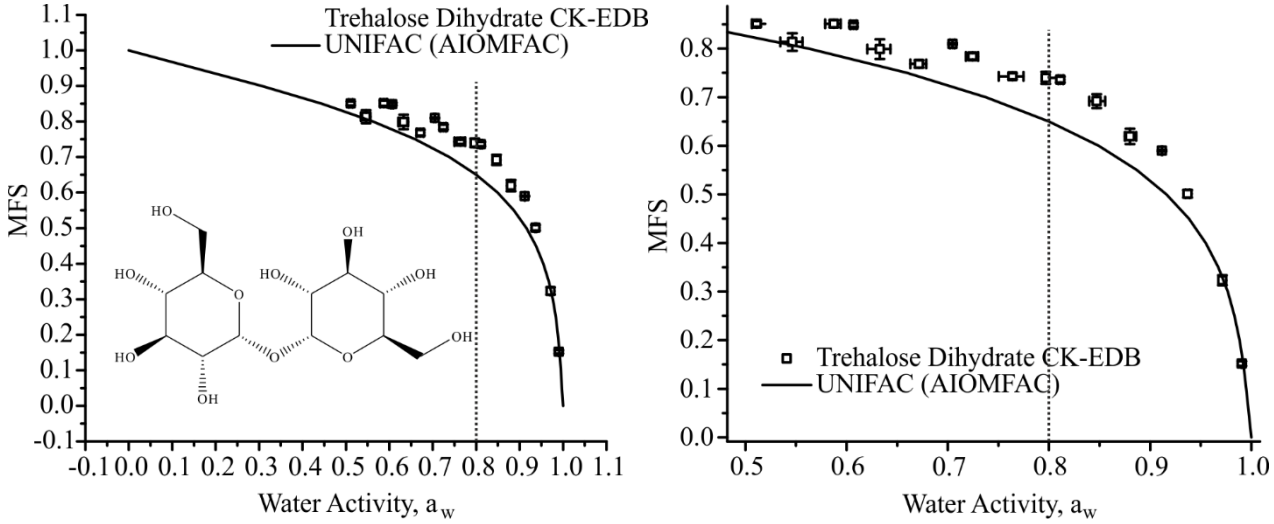

Table S30.1: Pure component refractive index (n_{melt}) determined using molar refraction where the melt density (ρ_{melt}) is determined using a polynomial fit of density to the square root of MFS ($MFS^{1/2}$ =x). Bulk values used are available in Cai et al. (2016). *Upper* and *lower* refer to 95 % confidence limits for fits to experimental data.

			Polynomial fit ($\rho_{sol} = a + b_1x + b_2x^2 + b_3x^3$)			
	n_{melt}	ρ_{melt}/ g.cm^{-3}	a	b_1	b_2	b_3
Best	1.5193	1.4682	997.8	8.2	284.3	177.8
Upper	1.5211	1.4734	997.8	11.6	269.79	194.19
Lower	1.5175	1.4629	997.8	4.87	298.84	161.43

Table S30.2: Tabulated experimental data points shown in **Fig S30.1.**

a_w	error a_w (+ve)	error a_w (-ve)	MFS	error MFS
0.51123	0.00397	0.0047	0.8511	0.00561
0.54636	0.01007	0.01196	0.81364	0.01816
0.5873	0.007	0.00844	0.85121	0.00732
0.60689	0.00263	0.00319	0.84879	0.00386
0.63303	0.01031	0.01244	0.79889	0.02031
0.67154	0.00716	0.00861	0.76858	0.00766
0.70479	0.00212	0.00262	0.80977	0.00199
0.72437	0.00577	0.00642	0.78413	0.00669
0.76384	0.01102	0.01364	0.743	0.00611
0.79679	0.00422	0.00225	0.7399	0.01219
0.81122	0.00282	0.00195	0.73624	0.0059
0.84712	0.00837	0.00721	0.69205	0.01427
0.88007	0.00598	0.00498	0.61945	0.01589
0.9118	5.25851E-4	5.4066E-4	0.58998	0.00159
0.93698	0.00204	0.00204	0.50101	0.00792
0.97142	0.00151	0.00149	0.3233	0.01015
0.99054	4.05516E-4	4.09208E-4	0.15195	0.00476

S31. Galactose Hygroscopicity

Fig S31.1: Hygroscopicity of (Sigma Aldrich ≥ 99 %), at 293.15 K. Open squares, these experiments; solid line, UNIFAC model. Data taken at RHs lower than indicated by the dashed black line show increased error in hygroscopicity retrieval due to the imposition of a kinetic limitation on water transport.

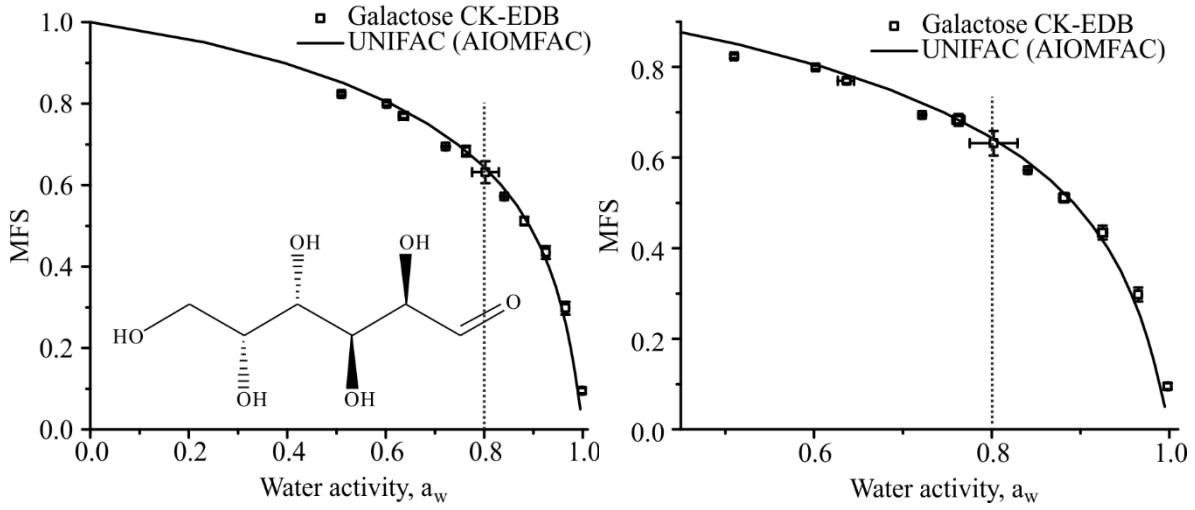

Table SI.31.1: Pure component refractive index (n_{melt}) is determined using molar refraction, assuming ideal mixing for calculation of the melt density (ρ_{melt}), from bulk data available in Cai et al. (2016). The variation of density as a function of the root of solute mass fraction ($MFS^{1/2} = x$) is represented by polynomial fit parameters. *Upper* and *lower* refer to 95 % confidence limits for fits to experimental data, (Section 2.2 in manuscript).

			Polynomial fit ($\rho_{sol} = a + b_1x + b_2x^2 + b_3x^3$)			
	n_{melt}	ρ_{melt}/ g.cm^{-3}	a	b_1	b_2	b_3
Best	1.5885	1.6306	997.36	403.27	83.09	150.11
Upper	1.5892	1.6351	996.67	165.3	-284.07	752.22
Lower	1.5878	1.6261	997.37	399.69	83.4	145.36

Table S31.2: Tabulated experimental data points shown in **Fig S31.1.**

a_w	error a_w (+ve)	error a_w (-ve)	MFS	error MFS
0.50996	0.00287	0.0034	0.82372	0.00382
0.60189	0.00267	0.00323	0.7993	0.00405
0.63684	0.00839	0.01012	0.76963	0.0055
0.72183	0.0016	0.00199	0.69438	0.00194
0.76282	0.00662	0.00694	0.68348	0.01289
0.80226	0.02704	0.02704	0.6317	0.02723
0.84064	0.00138	8.91966E-4	0.572	0.00141
0.88152	0.00559	0.00561	0.51157	0.01025
0.92485	0.00483	0.00491	0.43437	0.01532
0.96504	0.00377	0.00374	0.29773	0.01536
0.99822	0.00115	7.88489E-4	0.09505	0.00656

S32 Xylose Hygroscopicity

Fig S32.1: Hygroscopicity of (Sigma Aldrich ≥ 99 %), at 293.15 K. Open squares, these experiments; solid line, UNIFAC model.

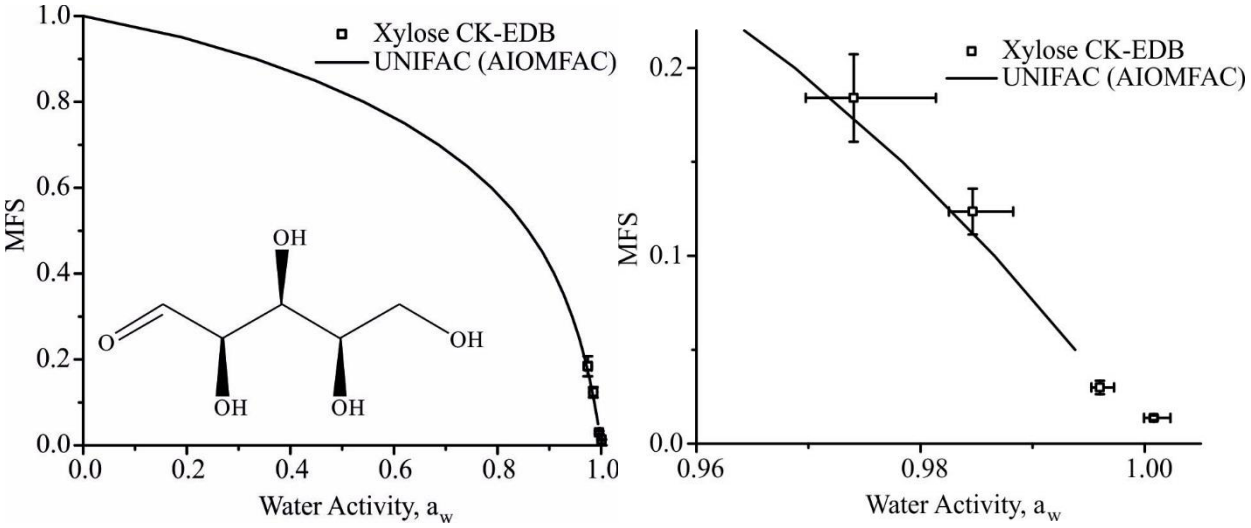

Table S32.1: Pure component refractive index (n_{melt}) is determined using molar refraction, assuming ideal mixing for calculation of the melt density (ρ_{melt}), from bulk data available in Cai et al. (2016). The variation of density as a function of the root of solute mass fraction ($MFS^{1/2} = x$) is represented by polynomial fit parameters. *Upper* and *lower* refer to 95 % confidence limits for fits to experimental data, (Section 2.2 in manuscript).

			Polynomial fit ($\rho_{sol} = a + b_1x + b_2x^2 + b_3x^3$)			
	n_{melt}	ρ_{melt}/ g.cm^{-3}	a	b_1	b_2	b_3
Best	1.5615	1.5626	996.73	127.69	-163.53	597.09
Upper	1.5619	1.5653	996.74	126.37	-159.45	591.57
Lower	1.5611	1.5598	996.72	128.97	-167.5	602.42

Table S32.2: Tabulated experimental data points shown in **Fig S32.1.**

a_w	error a_w (+ve)	error a_w (-ve)	MFS	error MFS
0.97404	0.00732	0.00429	0.1841	0.0233
0.98465	0.00361	0.00212	0.12356	0.01215
0.996	0.00127	7.43479E-4	0.02995	0.00361
1.00081	0.00148	8.71845E-4	0.01372	0.0012

S33 2,3-Dimethyl Succinic Acid Hygroscopicity

Fig S33.1: Hygroscopicity of 2,3-dimethyl succinic acid (Sigma Aldrich ≥ 99 %), at 293.15 K. Open squares, these experiments; solid line, UNIFAC model. (Density treatment for 2,2-dimethyl succinic acid used.)

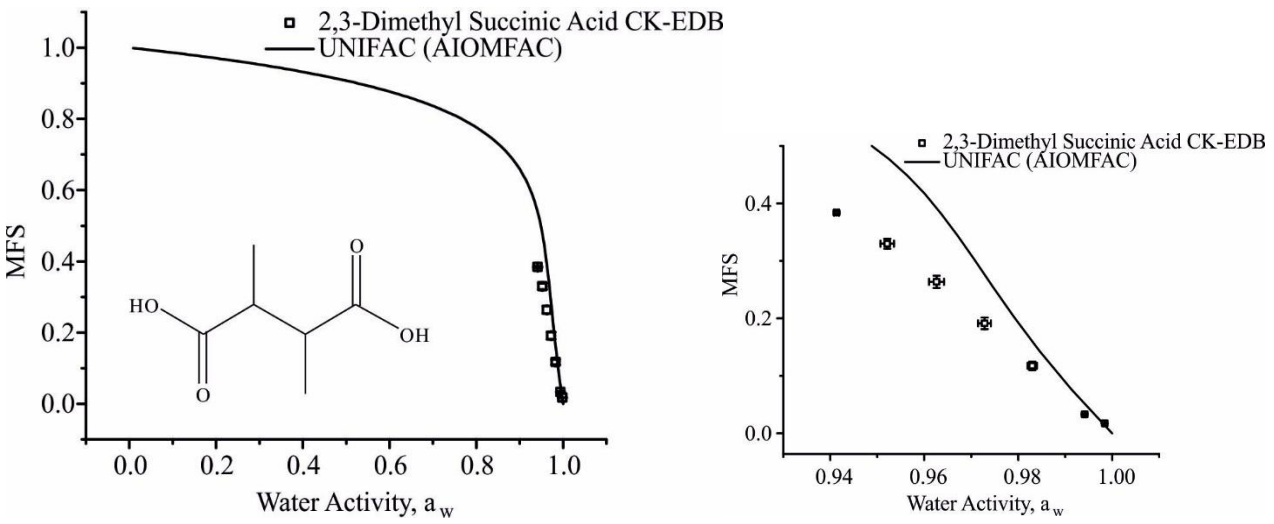

Table S33.2: Tabulated experimental data points shown in **Fig S33.1.**

a_w	error a_w (+ve)	error a_w (-ve)	MFS	error MFS
0.94132	5.11673E-4	5.12405E-4	0.38395	0.00207
0.95214	0.00144	0.00144	0.32979	0.00859
0.96262	0.00159	0.00159	0.26369	0.01065
0.97285	0.00138	0.00138	0.19135	0.01011
0.98303	0.001	0.001	0.11733	0.00731
0.99417	2.09751E-4	2.24291E-4	0.03301	0.00121
0.99844	2.59195E-4	4.09162E-4	0.01724	4.61378E-4

S34 Dimethyl Malonic Acid Hygroscopicity

Figure S34.1: Hygroscopicity of (Sigma Aldrich 98 %), at 293.15 K. Open squares, these experiments; solid line, UNIFAC model. (Density treatment for methyl succinic acid used.)

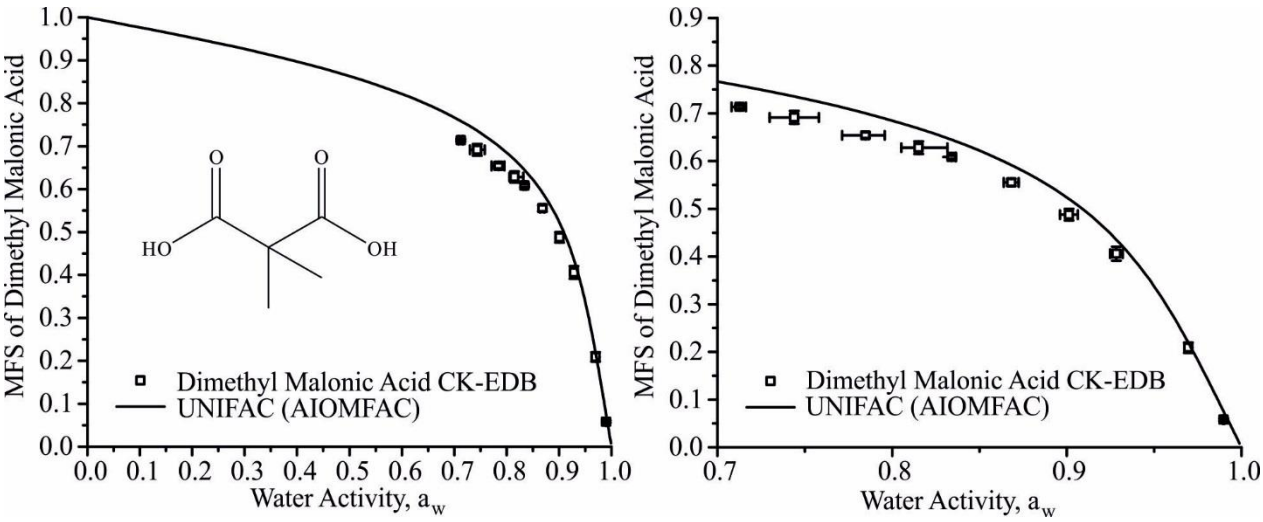

Table S34.2: Tabulated experimental data points shown in **Figure S34.1.**

a_w	error a_w (+ve)	error a_w (-ve)	MFS	error MFS
0.71262	0.00362	0.00449	0.7136	0.00301
0.744	0.0141	0.0141	0.69155	0.01343
0.78481	0.01088	0.01348	0.65412	0.00614
0.81516	0.01647	0.00985	0.62813	0.01311
0.83412	0.00246	0.00229	0.60844	0.00357
0.86818	0.00422	0.00426	0.5554	0.00729
0.90119	0.00509	0.00506	0.48761	0.01203
0.92833	0.00366	0.00365	0.40593	0.01475
0.96965	0.00157	0.00194	0.2089	0.01089
0.9897	4.75033E-4	4.76981E-4	0.05824	0.00271

S35 Aspartic Acid Hygroscopicity

Fig S35.1: Hygroscopicity of aspartic acid (Sigma Aldrich ≥ 99 %), at 293.15 K. Open squares, these experiments; solid line, UNIFAC model. (Density treatment for alanine used)

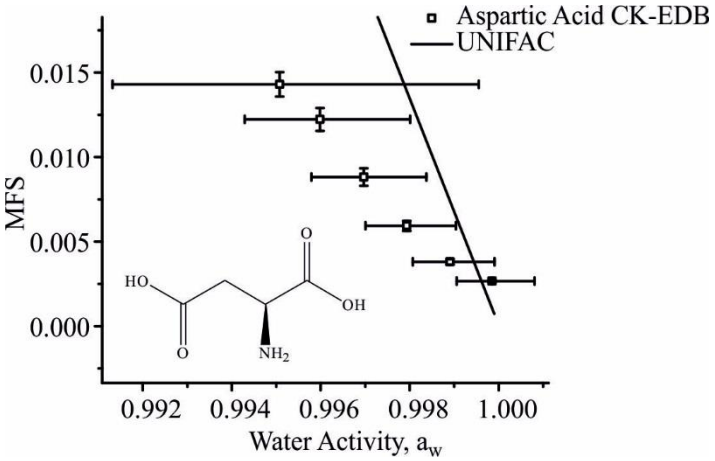

Table S35.1: Tabulated experimental data points shown in **Fig S35.1.**

a_w	error a_w (+ve)	error a_w (-ve)	MFS	error MFS
0.99507	0.00448	0.00375	0.01431	7.18E-04
0.99599	0.00202	0.0017	0.01223	6.83E-04
0.99697	0.00141	0.00118	0.00882	5.15E-04
0.99793	0.00111	9.28E-04	0.00594	3.01E-04
0.99891	0.001	8.39E-04	0.00381	1.64E-04
0.99985	9.52E-04	7.98E-04	0.00266	8.72E-05

S36 Asparagine Hygroscopicity

Fig S36.1: Hygroscopicity of asparagine (Sigma Aldrich ≥ 98 %), at 293.15 K. Open squares, these experiments; solid line, UNIFAC model. (Density treatment for alanine used)

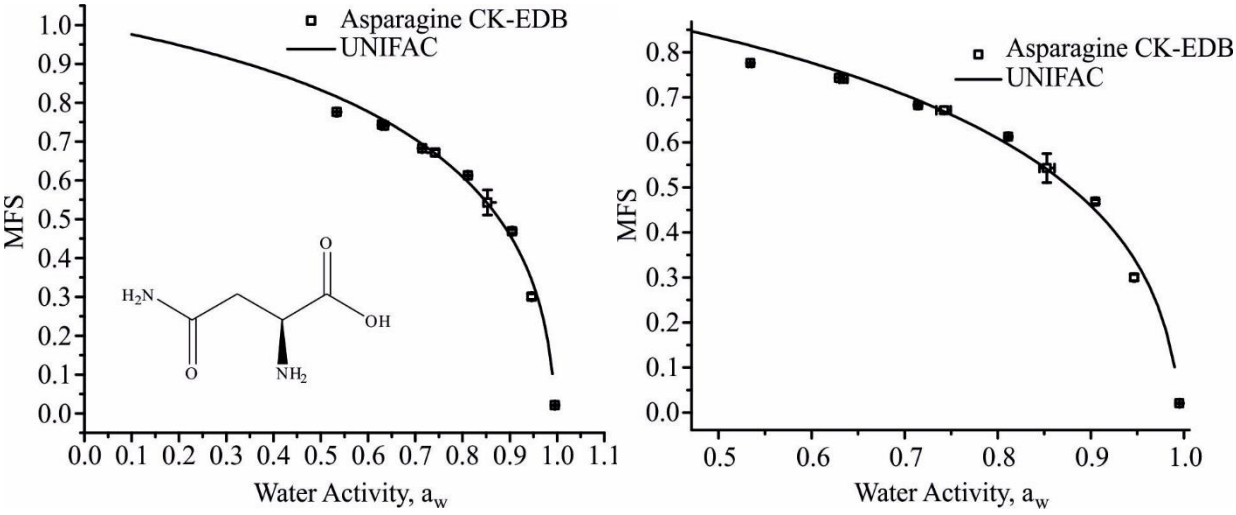

Table S36.1: Tabulated experimental data points shown in **Figure S36.1.**

a_w	error a_w (+ve)	error a_w (-ve)	MFS	error MFS
0.53409	0.00178	0.00213	0.77577	0.00129
0.62935	0.00189	0.0023	0.74326	0.00101
0.63444	0.00381	0.00465	0.74081	0.00101
0.71441	0.00113	0.0014	0.68254	0.00175
0.74237	0.007	0.00854	0.67146	0.00782
0.81123	8.45796E-4	8.49613E-4	0.61254	0.00185
0.85278	0.00812	0.00813	0.54286	0.03203
0.9048	0.00102	9.46055E-4	0.46853	0.00454
0.94641	0.00108	0.0011	0.3002	0.00693
0.9951	2.80427E-4	2.96722E-4	0.02083	0.00124

S37 Errors in Density and Refractive Index Parametrisations and their Impact on Hygroscopicity

Fig S37.1 Parametrisation for (a) density based on ideal mixing and bulk measured values for density up to the solubility limit and (b) refractive index predicted beyond the solubility limit using molar refraction. In both (a) and (b) dashed lines indicate the uncertainty envelope in the parametrisations. All bulk experimental values of aqueous density and refractive index are available in the supplementary information of Cai et al. (2016). In (c) measured equilibrium hygroscopicity curves are presented with upper and lower error envelope arising from the uncertainties in density and refractive index which is too small to be obvious.

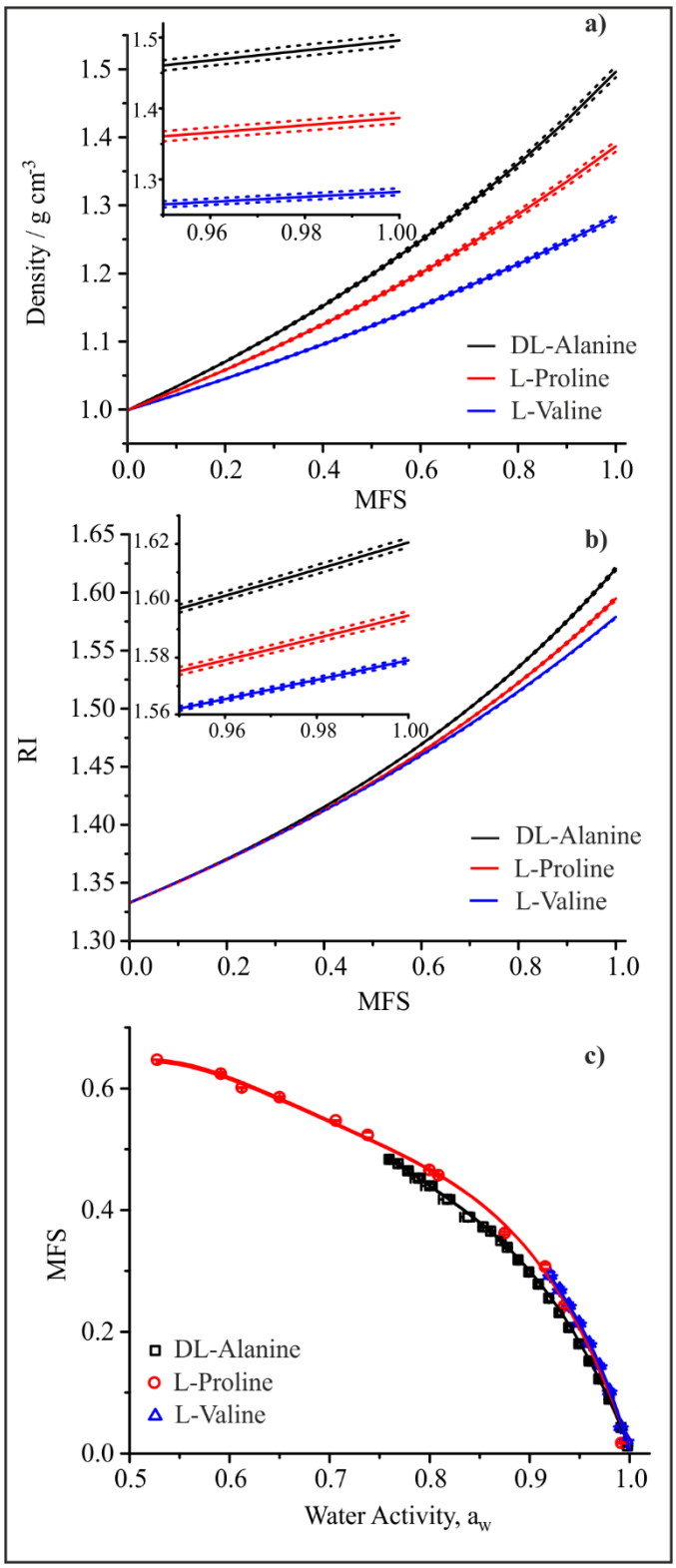
a)
Density / g cm^{-3}
MFS
DL-Alanine
L-Proline
L-Valine
b)
RI
MFS
DL-Alanine
L-Proline
L-Valine
c)
MFS
Water Activity, a_w
DL-Alanine
L-Proline
L-Valine

S38 ΔMFS for Simple Straight Chain Dicarboxylic Acids

Fig S38.1 The difference in mass fraction of solute (ΔMFS) between values predicted by UNIFAC and experimental values (a) oxalic acid, (b) malonic acid, (c) succinic acid and (d) glutaric acid.

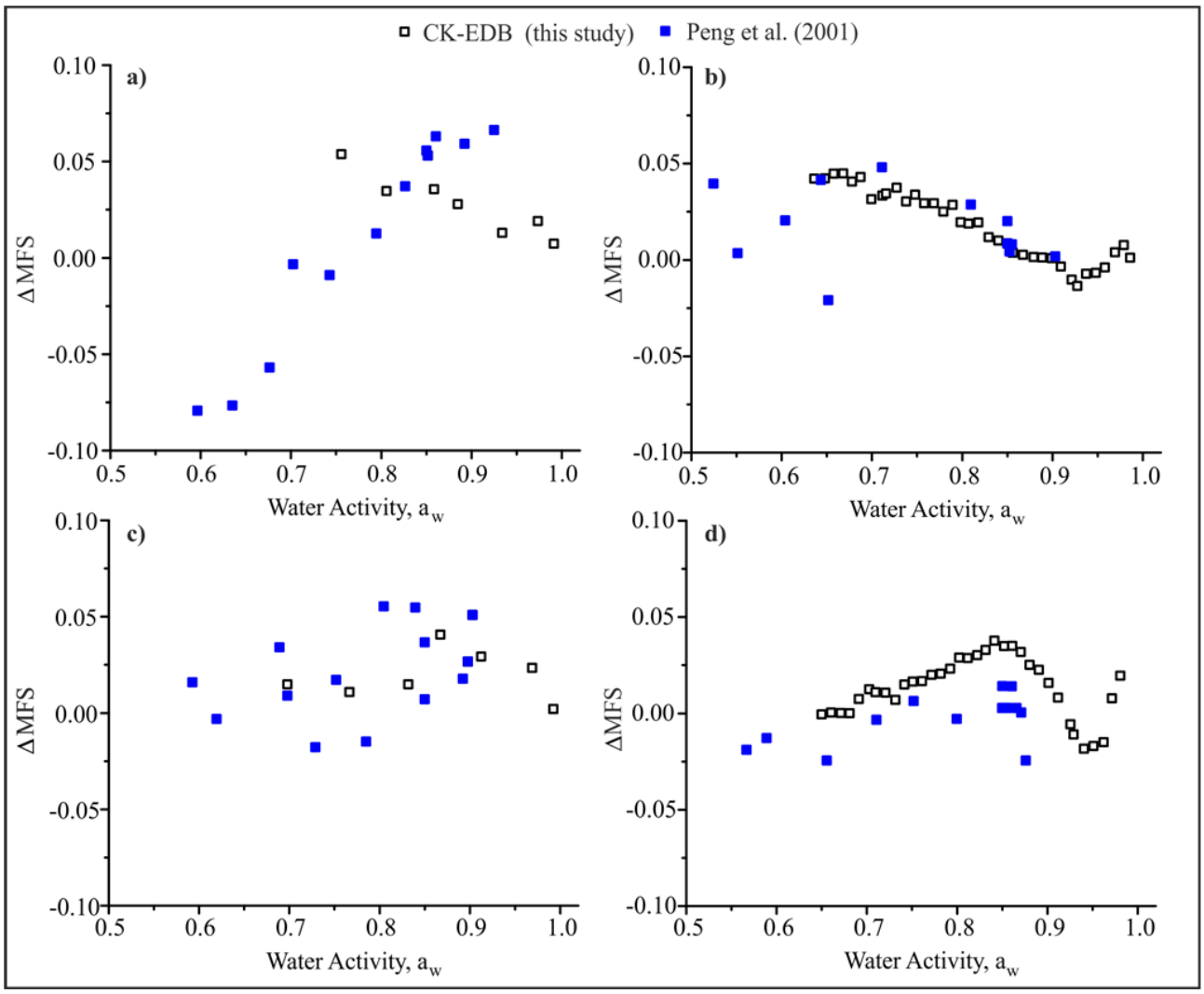

S39 Viscosity, Diffusion Constant and Timescale of Diffusional Mixing

The kinetic modelling framework used in the analysis of the droplet evaporation events is valid only in the absence of a bulk-kinetic limitation on near surface composition, i.e. the particle must be assumed to be homogeneous in composition. Such a limitation was obvious for hygroscopicity measurements of trehalose, galactose and sorbitol at RH's lower than 80 %. To ensure the measurements are not compromised by bulk diffusion, we consider two important factors.

Firstly, the impact of viscosity on the hygroscopicity retrievals becomes very obvious when we consider the consistency and uncertainty in the raw hygroscopic growth curves determined from different droplets evaporating into differing RHs. Droplets drying into different RHs reach different compositions at different times, and will retain different amounts of water because of different drying rates. This leads to an artificially low MFS at a particular RH which then slowly returns to the equilibrium curve overtime. Thus, an inconsistency is apparent between retrieved hygroscopic growth curves (or MFS vs a_w) when drying into different RHs. An example of this is shown in Figure S39.1, where we report unbinned hygroscopicity data for alanine (a non-viscous amino acid) and trehalose (viscous at RHs lower than 80%). It is clear here that the different portions of the hygroscopic curves retrieved from measurements at different RHs are consistent for alanine but not for trehalose. A further easy way to identify this retention of water in a particle that is not fully

equilibrated is simply to measure the much longer time-dependence in size once the initial evaporation of water has stopped. In droplets that have reached a bulk diffusion limitation, the existence of a kinetic limitation is apparent in a steadily decreasing size as water continues to leave over a timescale longer than 10 s.

Fig S39.1 a) Unbinned hygroscopicity data for the compound alanine. b) Unbinned hygroscopicity data for the compound trehalose. At 50 % RH trehalose has a viscosity of 3.8 x 10^5 Pa.s (Song et al. 2016).

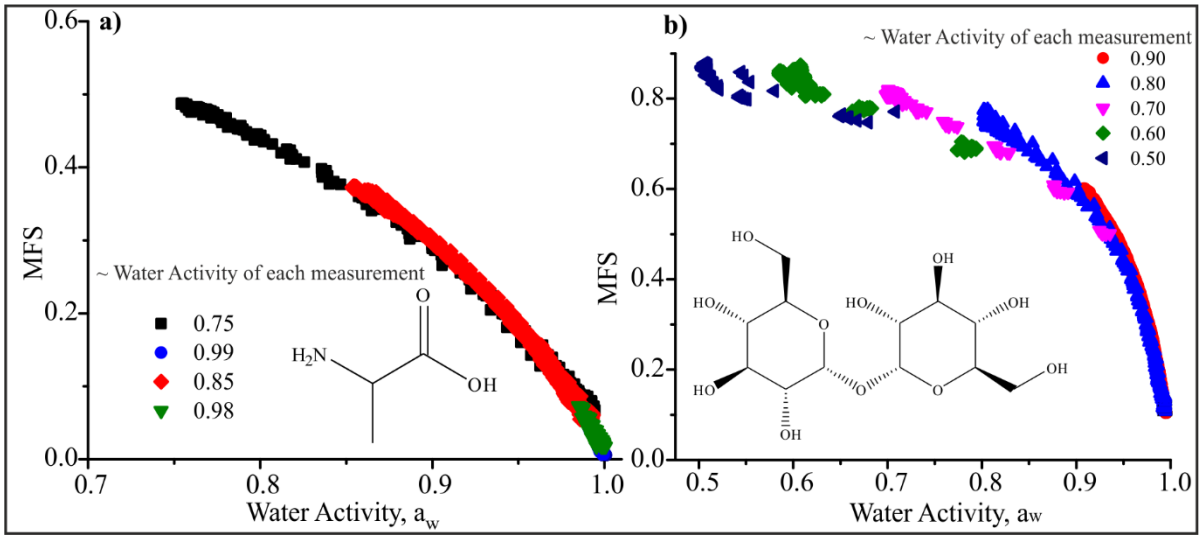

Secondly, we can determine the expected conditions under which we might expect problems to arise in retrieving hygroscopic growth curves from an evaporation measurement. Considering again trehalose at 80 % RH, an aqueous-trehalose droplet has a viscosity of 0.5 Pa.s, increasing to 3.8×10^5 Pa.s at 50 % RH (Song et al. 2016). Therefore, as the RH of the gas phase for the evaporation measurement is lowered, we can expect the increasing viscosity/decreasing diffusivity to become increasingly important. By contrast, for aqueous-carboxylic acid droplets, the viscosity never gets above 1 Pa s even at the driest RHs considered here (Song et al. 2016).

With these known dependencies of viscosity on water activity, we can estimate the timescale for diffusional mixing within a droplet, assuming that this provides an estimate of the timescale for an evaporating droplet to form a homogeneous mixture. This timescale must be considerably shorter than the evaporation timescale for our hygroscopicity estimations to be valid. First, the Stokes-Einstein equation is used to estimate the diffusion constant of water at varying viscosity (varying RH).

$$D = \frac{k_B T}{6\pi r_{mol} \eta} \qquad (1.1)$$

D is the diffusion constant, k_B is the Boltzmann constant, T is temperature, r_{mol} is the molecular radius of water (taken as 1.375 Å) and η is the viscosity. It should be noted that equation (1.1) is likely to provide a significant underestimate of the diffusion constant due to the failure of the Stokes-Einstein equation. At a viscosity of 100 Pa s, the diffusion constant for water in sucrose is already more than one order of magnitude larger than estimated from the viscosity (Power et al. 2013). However, using diffusion constants estimated from (1.1) will provide an upper limit on the diffusional mixing timescale. The timescale for diffusional mixing, τ, is then estimated using the expression

$$\tau = \frac{a^2}{\pi^2 D} \qquad (1.2)$$

where a is the droplet radius (set as 10 microns in this calculation).

We compare the diffusional mixing timescales for aqueous droplets of trehalose, NaCl, $NaNO_3$ and glutaric acid in the newly added supplemental Figure S39.2 (and repeated below). Given that we have been able to report accurate hygroscopic growth curves for $NaNO_3$ down to 50 % RH (see Rovelli et al. 2016 and the

response to referee 2), it is clear that a final viscosity at 50 % of ~ 0.1 Pa.s (Baldelli et al.) is insufficient to impede accurate measurement of the hygroscopicity. Indeed, this suggests that water transport in any aerosol droplet that maintains a viscosity lower than 0.1 Pa.s during drying should remain sufficiently fast to avoid a bulk diffusion limitation, permitting accurate hygrosocpicity measurements. As an example of the diacarboyxlic acids considered in this study, glutaric acid has a considerably lower viscosity at 50 % RH of ~ 0.01 Pa.s (Song et al. 2016), indicative of what we might expect for all such similar systems. By contrast, aqueous-trehalose droplets cross the 0.1 Pa.s viscosity threshold at a water activity of ~0.85 (Song et al. 2016), commensurate with the deviation and increased scatter in the hygroscopicity measurements reported above for this compound.

Based on the two considerations above and to indicate clearly the water activity ranges over which we consider the hygroscopicity measurements to be valid for trehalose (S30), galactose (S31) and sorbitol (S29), we have added a dashed line to indicate where the data appear to become kinetically limited. We have added the following words to the captions of these Figures: "Data taken at RHs lower than indicated by the dashed black line show increased error in hygroscopicity retrieval due to the imposition of a kinetic limitation on water transport."

Fig S39.2 a) Viscosity of Trehalose, NaCl, NaNO3 and Glutaric Acid as a function of RH. b) Estimated diffusion constant as a function of RH. c) Timescale for diffusional mixing at the RH shown on x-axis. Dashed green line represents 1 second timescale for diffusional mixing.

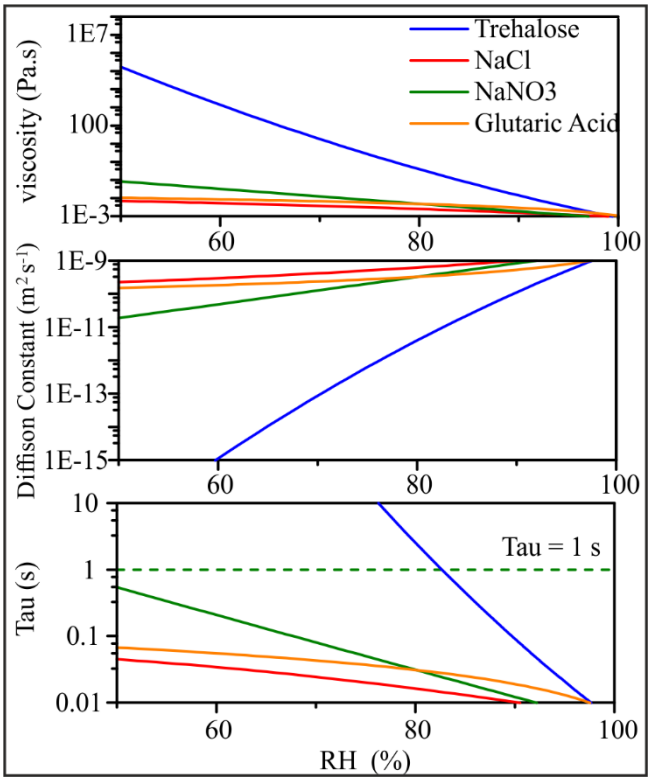

A. Baldelli, R. M. Power, R. E. H. Miles, J. P. Reid and R. Vehring *Effect of crystallization kinetics on the properties of spray dried microparticles*, Aerosol Science and Technology, 2016, 50:7, 693-704, DOI:10.1080/02786826.2016.1177163

R. M. Power, S. H. Simpson, J. P. Reid and A. J. Hudson, *The transition from liquid to solid-like behaviour in ultrahigh viscosity aerosol particles*, Chemical Science, 2013, 4 , 2597, DOI: 10.1039/c3sc50682g

Y. Chul Song, A. E. Haddrell, B. R. Bzdek, J. P. Reid, T. Bannan, D. O. Topping,, C. Percival, and C. Cai *Measurements and Predictions of Binary Component Aerosol Particle Viscosity* J. Phys. Chem. A 2016, 120, 8123−8137, DOI: 10.1021/acs.jpca.6b07835

S40 Differences between Cyclic and Open Chain Sugar Conformer Thermodynamic Predictions

Table S40.0: Table of UNIFAC groups for cyclic and open chain galactose and xylose.

Compound	Open Chain (In Manuscript)	Cyclic
Galactose	$CHO\ (CH_1^{(OH)})_4\ CH_2^{(alc)}\ (OH)_5$	$(CH^{[alc]})_4(CH_2^{[OH]})(CHO^{[ether]})(OH)_4$
Xylose	$(CH_2(OH))_3\ CH_2^{(alc)}\ CHO\ (OH)_4$	$(CH^{[OH]})_4(CHO^{[ether]})(OH)_4$

Figure S40.0 Galactose and Xylose CK-EDB data as a function of MFS and water activity compared with predictions for both cyclic and open chain UNIFAC group thermodynamic predictions